INL/EXT-11-23379

# MPACT FY2011 Advanced Time-Correlated Measurement Research at INL

D. L. Chichester
S. A. Pozzi
J. L. Dolan
M. Flaska
S. M. Watson


September 2011

**INL is a U.S. Department of Energy National Laboratory operated by Battelle Energy Alliance**

**DISCLAIMER**

This information was prepared as an account of work sponsored by an agency of the U.S. Government. Neither the U.S. Government nor any agency thereof, nor any of their employees, makes any warranty, expressed or implied, or assumes any legal liability or responsibility for the accuracy, completeness, or usefulness, of any information, apparatus, product, or process disclosed, or represents that its use would not infringe privately owned rights. References herein to any specific commercial product, process, or service by trade name, trade mark, manufacturer, or otherwise, do not necessarily constitute or imply its endorsement, recommendation, or favoring by the U.S. Government or any agency thereof. The views and opinions of authors expressed herein do not necessarily state or reflect those of the U.S. Government or any agency thereof.

INL/EXT-11-23379

# MPACT FY2011 Advanced Time-Correlated Measurement Research at INL

D. L. Chichester[1], S. A. Pozzi[2], J. L. Dolan[1,2], M. Flaska[2], and S. M. Watson[1]

[1] Idaho National Laboratory
[2] Department of Nuclear Engineering & Radiological Sciences,
University of Michigan

September 2011

Idaho National Laboratory
Idaho Falls, Idaho 83415

http://www.inl.gov

Prepared for the
U.S. Department of Energy
Office of Nuclear Energy
Under DOE Idaho Operations Office
Contract DE-AC07-05ID14517

## ACKNOWLEDGEMENT

The authors would like to kindly acknowledge the in-kind support of Dr. Paolo Peerani, his research colleagues Dr. Alice Tomanin and Mr. Santino Frison, and other staff at the European Commission's PERLA Laboratory at the Joint Research Center in Ispra, Italy. Without his interest in our work, his desire to collaborate with our research team, and his support in hosting us at his laboratory, none of the work that took place at JRC-Ispra in 2011 would have been possible. The research collaboration is also thankful to Dr. Giancarlo Nebia and Dr. Giuseppe Viesti of the Galileo Galilei Department of Physics at the University of Padova, for allowing us to borrow the associated-particle electronic neutron generator used for the experiments.

The authors would also like to acknowledge and thank the staff at INL's Materials and Fuels Complex and the ZPPR facility for their support and enthusiasm for the experiments described in this report. In particular, we would like to acknowledge the helpful assistance of shift supervisor Robert Neibert and his staff at ZPPR for their assistance in working to support the imaging experiments carried out by the ORNL team at ZPPR in August, 2011.

The authors would also like to acknowledge and thank Dr. Mark Mullen, technical director for the MPACT program, for his ongoing support of this research project.

The work in this report was sponsored by the U.S. Department of Energy's Fuel Cycle Research and Development program and its Materials Protection, Accounting, and Control Technologies (MPACT) program.

# EXECUTIVE SUMMARY

Simulations and experiments have been carried out to investigate advanced time-correlated measurement methods for characterizing and assaying nuclear material for safeguarding the nuclear fuel cycle. These activities are part of a project studying advanced instrumentation techniques in support of the U.S. Department of Energy's Fuel Cycle Research and Development program and its Materials Protection, Accounting, and Control Technologies (MPACT) program. For fiscal year 2011 work focused on examining the practical experimental aspects of using a time-tagged, associated-particle electronic neutron generator for interrogating low-enrichment uranium in combination with steady-state interrogation using a moderated $^{241}$Am-Li neutron source. Simulation work for the project involved the use of the MCNP-PoliMi Monte Carlo simulation tool to determine the relative strength and the time-of-flight energy spectra of different sample materials under irradiation. Work also took place to develop a post-processor parser code to extract comparable data from the MCNP5&6 codes. Experiments took place using a commercial deuterium-tritium associated-particle electronic neutron generator to irradiate a number of uranium-bearing material samples. Time-correlated measurements of neutron and photon signatures of these measurements were made using five liquid scintillator detectors in a novel array, using high-speed waveform digitizers for data collection. This report summarizes the experiments that took place in FY2011, presents preliminary analyses that have been carried out to date for a subpart of these experiments, and describes future activities planned in this area. The report also describes support Idaho National Laboratory gave to Oak Ridge National Laboratory in 2011 to facilitate 2-dimensional imagery of mixed-oxide fuel pins for safeguards applications as a part of the MPACT program.

# CONTENTS

# FIGURES

## TABLES

# MPACT FY2011 Advanced Time-Correlated Measurement Research at INL

## 1 INTRODUCTION

This report documents work performed by Idaho National Laboratory in fiscal year (FY) 2011 to evaluate the use of time-tagged, active neutron interrogation with an associated particle (AP) electronic neutron generator (ENG), and active neutron interrogation with a low-energy $^{241}$AmLi-based neutron source, for characterizing nuclear material for nuclear safeguards applications. This work included the development of new modeling tools, the creation of pre-experiment and post-experiment simulations, and the design and assembly of a liquid-scintillator based data acquisition system including hardware and software tools. The experiments for this effort took place in May, 2011. As of the end of FY2011 preliminary simulations have been carried out to address the AP-ENG aspects of the experiments, which are reported here. Further work is yet to be done to simulate the AmLi interrogation measurements, and to integrate data from both sets of experiments.

Also in FY2011, INL supported collaborators from Oak Ridge National Laboratory (ORNL) in the execution of an experimental campaign at INL's Materials and Fuels Complex (MFC), in the ZPPR facility (formerly known as the zero-power physics reactor). This report also includes details of the support activities undertaken for this experiment.

### 1.1 Background – The INL and University of Michigan Collaboration

INL has been working to explore new methods for analyzing nuclear materials using fast, time-correlated measurements for several years.[1] This work, supported by the U.S. Department of Energy's Fuel Cycle Research and Development program and it's Materials Protection, Accounting, and Control Technologies (MPACT) program, has been a collaborative effort including staff at INL as well as staff and students in the Department of Nuclear Engineering & Radiological Sciences at the University of Michigan. These activities have included simulation and modeling using the MCNP-PoliMi Monte Carlo simulation tool and experiments to validate the simulations, development of hands-on experimental methods, and the discovery of pitfalls and challenges in performing these types of measurements that cannot be identified any other way. INL possess a strong background in theses areas, notably addressing nuclear security and safeguards challenges, heavily weighted towards real world experiments and system-level development and demonstration efforts, and the use of ENGs in active neutron interrogation. The University of Michigan team is a recognized world leader in the study and development of the MCNP-PolliMi computer code for modeling time-correlated measurements, as well as in the use of liquid-scintillator-based detector systems for studying and characterizing special nuclear materials and their time-correlated signatures.

## 1.2 Background – Fuel Cycle Materials

As described in the FY2009 End-of-Year Report, advanced nuclear fuels are currently under development within the Department of Energy's Fuel Cycle Research and Development program as part of a long-term research effort focused at understanding the behavior of mixed-oxide (MOX) fuels containing minor actinides and long-lived fission products.[1] The aim of this work is to understand how these materials impact the long-term performance of nuclear fuel in order to be able to design and manufacture advanced fuels for use in next-generation reactors. Reusing, or recycling, the higher actinides and long-lived fission products in advanced nuclear fuels ultimately leads to the transmutation of these materials into shorter-lived waste products which may be more easily and more safely disposed of. There are several potential benefits of reusing nuclear fuel including the reclamation of additional energy content from once-through used fuels, the reduction or removal of longer-lived waste products from spent fuel, and the lessening of the storage demands eventually placed on facilities for the long-term storage or disposal of spent fuels. In parallel with the fuel development projects research and development is also underway to develop advanced fuel reprocessing approaches to produce these fuels and to develop advanced reactors to use these fuels. However, in addition to these core engineering research and development projects the ultimate viability of these new technology developments will be critically linked to advances in nuclear safeguards and material protection, accounting, and control technologies (MPACT).

Traditional nuclear safeguard measurement techniques used to monitor uranium oxide fuels are not well-suited for analyzing advanced MOX fuels. Gross gamma-ray counting is complicated by the presence of the additional radioactive materials in the fuel while high-resolution gamma-ray spectroscopy can be difficult to perform due to the presence of multiple interferences associated with the presence of the minor actinides. Similarly, the powerful passive and active neutron-based nondestructive assay techniques used with current-generation fresh and irradiated commercial nuclear fuel are complicated by the presence of multiple higher actinides, some of which have spontaneous fission and induced fission signatures comparable to plutonium. From 2009 through 2011 it has been the goal of the INL-University of Michigan collaboration to explore techniques for fast-neutron and photon-correlation measurements, both passively and with active interrogation. The aim of these efforts has been to improve the fundamental understanding of nuclear materials and the physics of detection methods through coupled theory, simulation, and experiment, as necessary to develop next-generation materials management and MPACT technology. More broadly speaking, these efforts have been part of the larger MPACT research portfolio seeking to enhance overall nuclear fuel cycle proliferation resistance via improved technologies for used fuel management.

Important aspects of long-term, science-based, engineering-driven research and development (R&D) include small-scale experiments, theory development, and advanced modeling and simulation with validation experiments. This project embraces this paradigm for the "science-based" R&D approach for improving domestic MPACT approaches for security and safeguards.

# 2 The 2011 Experimental Campaign

Work in FY2011 started in January with the conceptual development of an experimental campaign to explore how a time-tagged, AP-ENG might be used in combination with fast-neutron measurement techniques to characterize special nuclear material (SNM) for material protection, accounting, and control applications. In FY2009 the research team performed passive fast-neutron measurement experiments with MOX fuel at INL's ZPPR facility. For FY2011 we took advantage of an offer from Dr. Paolo Peerani of the European Commissions' Joint Research Center (JRC) in Ispra, Italy to use their facilities and materials for our research. This was particularly useful because they possess low-enrichment uranium samples not available at INL. Uranium analysis is particularly well suited for active interrogation examinations due to the low inherent neutron emission source term of this material, which makes it particularly difficult to characterize using passive neutron measurements methods. Concurrently, we also accepted an offer to borrow a next generation, state-of-the-art AP-ENG device from Dr. Giancarlo Nebia and Dr. Giuseppe Viesti of the Galileo Galilei Department of Physics at the University of Padua, Padua, Italy.

## 2.1 Materials

At JRC-Ispra three distinct sets of measurements were performed. First, testing was done using, separately, three stainless-steel cylinders filled with uranium yellowcake ($U_3O_8$). A photograph of one of the containers is shown in Figure 1. One container, LU11, held 1.68418 kg of uranium with a $^{235}U$ enrichment of 1%. The second container, LU25, held 2.36376 kg of uranium with a $^{235}U$ enrichment of 3.1%. The third container, LU44, held 2.36376 kg of uranium with a $^{235}U$ enrichment of 5%. Information about these containers, including dimensions for the cans, is presented in Figure 2.

The second set of tests involved using, simultaneously, three metal-alloy plutonium pellets. The first pellet, PM1, contained 12.5 ± 0.3 g of plutonium with 95.39377% $^{239}Pu$. The second pellet, PM2, contained 18.8 ± 0.4 g of plutonium with 95.46608% $^{239}Pu$. The third pellet, PM3, contained 18.98 ± 0.7 g of plutonium with 91.28147% $^{239}Pu$. The container for PM1 had an outer diameter of 1.4 cm, the container for PM2 had an outer diameter of 1.6 cm, and the container for PM3 had an outer diameter of 1.9 cm. All three pellets were in aluminum cylinders having a height of 4.6 cm. Full details for these three items are presented in Figure 3 through Figure 5.

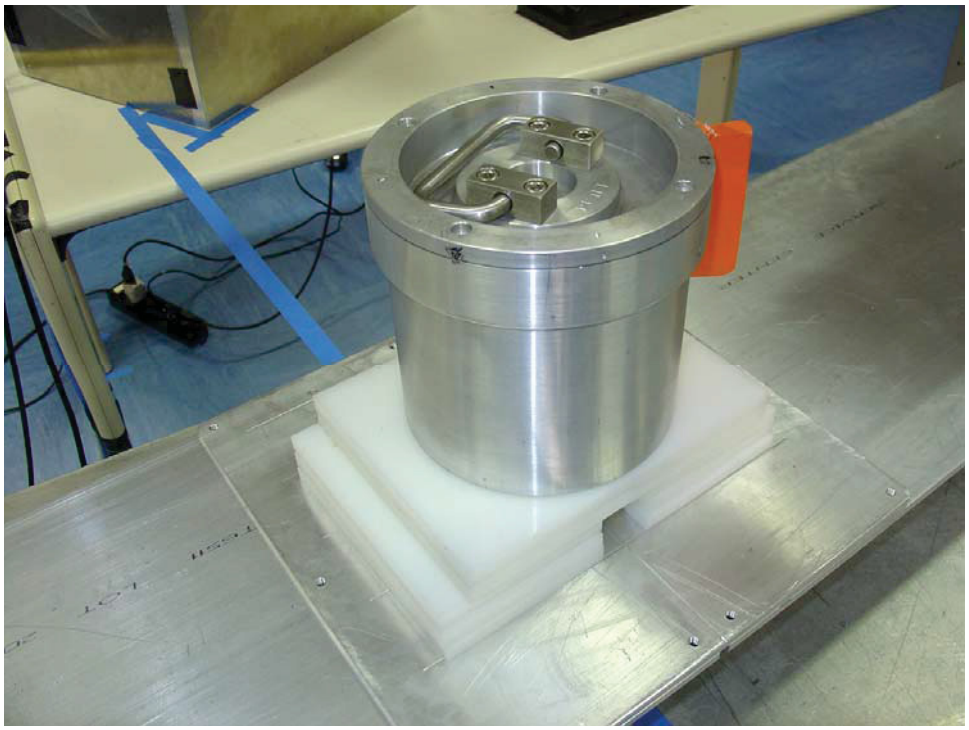

**Figure 1 Photograph of one of the uranium-oxide storage containers.**

## Table 2 Proposal 2 LEU powder standard FBFC

| Identification | 235U (%) | U3O8 (g) | U (g) | 235U (g) | Container model | Fill Height (mm) |
|---|---|---|---|---|---|---|
| LU 11 | 1 | 1995 | 1684,18 | 16,84 | ~~A3~~ B1 | 152 |
| LU 12 | | 2800 | 2363,76 | 23,64 | A3 | 262 |
| LU 13 | | 7045 | 5947,39 | 59,47 | B2 | 262 |
| Total | | 11840 | 9995,33 | 99,95 | | |
| LU 21 | 3,1 | 530 | 447,43 | 13,87 | A1 | 49,5 |
| LU 22 | | 1112 | 938,75 | 29,10 | ~~A2~~ A2 | 104 |
| LU 23 | | 1333 | 1125,32 | 34,88 | B1 | 49,5 |
| LU 24 | | 1680 | 1418,26 | 43,97 | A3 | 152 |
| LU 25 | | 2800 | 2363,76 | 73,28 | ~~A3~~ B1 | 262 |
| LU 26 | | 2800 | 2363,76 | 73,28 | B1 | 104 |
| LU 27 | | 2800 | 2363,76 | 73,28 | C1 | 49,5 |
| LU 28 | | 4000 | 3376,80 | 104,68 | B2 | 149 |
| LU 29 | | 5881 | 4964,74 | 153,91 | C1 | 104 |
| LU 30 | | 7045 | 5947,39 | 184,37 | B2 | 262 |
| LU 31 | | 8480 | 7158,82 | 221,92 | B2 | 315 |
| LU 32 | | 14800 | 12494,16 | 387,32 | C2 | 262 |
| LU 33 | | 17810 | 15035,20 | 466,09 | C2 | 315 |
| Total | | 71071 | 59998,14 | 1859,94 | | |
| LU 41 | 5 | 320 | 270,14 | 13,51 | A1 | 29,9 |
| LU 42 | | 1170 | 987,71 | 49,39 | A2 | 110 |
| LU 43 | | 1630 | 1376,05 | 68,80 | A3 | 154 |
| LU 44 | | 2800 | 2363,76 | 118,19 | ~~A3~~ B1 | 262 |
| Total | | 5920 | 4997,65 | 249,88 | | |
| | | | | 2209,77 | | |

| Container Model | Material | Inter.Ø (mm) | Exter. Ø (mm) | Max Vol. (cm³) | Max.U3O8 (Kg) | Max. Ht. Fiss (mm) | Ht. Container (mm) |
|---|---|---|---|---|---|---|---|
| A1 | A.G.3M | 87 | 95 | 480 | 0,8 | 75 | 92,5 |
| A2 | A.G.3M | 87 | 95 | 800 | 1,3 | 125 | 152,5 |
| A3 | A.G.3M | 87 | 95 | 1650 | 2,8 | 275 | 302,5 |
| B1 | A.G.3M | 138 | 158 | 1700 | 3,1 | 116,5 | 148,5 |
| B2 | A.G.3M | 138 | 158 | 4700 | 8,48 | 315 | 350 |
| C1 | A.G.3M | 200 | 220 | 3600 | 6,4 | 116,5 | 148,5 |
| C2 | A.G.3M | 200 | 220 | 9800 | 17,81 | 315 | 350 |

Density used : 1,8 g/cm³

**Figure 2 LEU powder samples used at JRC-Ispra.**

R. Berndt, P. Montreau
IPSC, Non-Proliferation and Nuclear Safeguards Unit,
Gamma Sector

Ispra, 08. 03. 02

## PERLA sample PM1

(ex CPZA1038 container3)

### Pu metal alloy pellet

| | | |
|---|---|---|
| **Material:** | Pu Ni Cu alloy | (official declaration of former owner towards the IAEA: "Pu metal") |
| **Shape, size:** | cylinder | diameter: 7.5 ± 0.1 mm<br>length: 15.5 ± 0.1 mm |
| **Pellet mass:** | (13.7 +- 0.1) g | |
| **Pu mass:** | (12.5 +- 0.3) g | |
| **Pu mass factor:** | (91.0 +- 2.1) % | |
| **Ni mass factor:** | ( 5.5 +- 1.0) % | |
| **Cu mass factor:** | ( 3.5 +- 1.0) % | |
| **Density:** | (20.0 +- 0.3) % g/cm$^3$ | |

**Isotopic composition:**

Composition at the 01. 01. 2001(declaration date):

| Isotope | wt% | relative measurement error / % | |
|---|---|---|---|
| 238Pu | 0.00412 | 9.87 | |
| 239Pu | 95.39377 | 0.03 | |
| 240Pu | 4.53195 | 0.72 | |
| 241Pu | 0.05501 | 1.03 | |
| 242Pu | 0.0151 | (10) | calculated with „new algorithm" |
| 241Am | 0.22599 | 0.44 | |

**Containers:**

| | | | |
|---|---|---|---|
| 1. Outside container: | PERLA mod 5 no. 10A | | |
| | gross mass of the container with label: | | 245.2 +- ... g |
| 2. PVC bag: | 1.4 g | | |
| 3. Al capsule: | cylindrical container | | |
| | outside diameter: | 14 mm | |
| | outside length: | 46 mm | |
| | side wall thickness: | 3 mm | |
| | bottom thickness: | 5 mm | (with 2 mm slot for screw driver) |
| | plug thickness: | 8 mm | (with 2 mm slot for screw driver) |
| | Al tightning disk: | 2 mm | |
| | total Al mass: | (14.50 ± 0.05) g | |

**Figure 3 Pu sample PM1 at JRC-Ispra.**

R. Berndt, P. Mortreau
IPSC, Non-Proliferation and Nuclear Safeguards Unit,
Gamma Sector

Ispra, 08. 03. 02

## PERLA sample PM2

(ex CPZA1038 container1)

## Pu metal alloy pellet

**Material:** Pu Ni Cu alloy (official declaration of former owner towards the IAEA: "Pu metal")

**Shape, size:** cylinder diameter: 10.0 ± 0.1 mm; length: 13.2 ± 0.1 mm

**Pellet mass:** (20.5 +- 0.1) g

**Pu mass:** (18.8 +- 0.4) g

**Pu mass factor:** (91.7 +- 2.2) %
**Ni mass factor:** ( 5.1 +- 1.0) %
**Cu mass factor:** ( 3.2 +- 1.0) %

**Density:** (19.7 +- 0.3) % g/cm$^3$

**Isotopic composition:**

Composition at the 01. 01. 2001(declaration date):

| Isotope | wt% | relative measurement error / % | |
|---|---|---|---|
| 238Pu | 0.00426 | 8.22 | |
| 239Pu | 95.46608 | 0.03 | |
| 240Pu | 4.45799 | 0.64 | |
| 241Pu | 0.05703 | 0.89 | |
| 242Pu | 0.0146 | (10) | calculated with „new algorithm" |
| 241Am | 0.21472 | 0.40 | |

**Containers:**

1. Outside container: PERLA mod 5 no. 8A
   gross mass of the container with label: 255.6 +- ... g
2. PVC bag: 1.6 g
3. Al capsule: cylindrical container

| | | |
|---|---|---|
| outside diameter: | 16 mm | |
| outside length: | 46 mm | |
| side wall thickness: | 3 mm | |
| bottom thickness: | 5 mm | (with 2 mm slot for screw driver) |
| plug thickness: | 8 mm | (with 2 mm slot for screw driver) |
| Al tightning disk: | 2 mm | |
| total Al mass: | (17.73 ± 0.05) g | |

**Figure 4 Pu sample PM2 at JRC-Ispra.**

R. Berndt, P. Mortreau
IPSC, Non-Proliferation and Nuclear Safeguards Unit,
Gamma Sector

Ispra, 08. 03. 02

## PERLA sample PM3

(ex CPZA1038 container6)

## Pu metal alloy pellet

| | | |
|---|---|---|
| **Material:** | Pu Ni Cu alloy | (official declaration of former owner towards the IAEA: "Pu metal") |
| **Shape, size:** | cylinder | diameter: 11.45 ± 0.1 mm<br>length: 11.45 ± 0.1 mm |
| **Pellet mass:** | (20.1 +- 0.2) g | |
| **Pu mass:** | (18.9 +- 0.7) g | |
| **Pu mass factor:** | (94.0 +- 3.8) % | |
| **Ni mass factor:** | ( 1.7 +- 0.5) % | |
| **Cu mass factor:** | ( 4.3 +- 1.0) % | |
| **Density:** | (22.4 +- 0.3) % g/cm$^3$ | |

**Isotopic composition:**

Composition at the 01. 01. 2001(declaration date):

| Isotope | wt% | relative measurement error / % |
|---|---|---|
| 238Pu | 0.02708 | 2.37 |
| 239Pu | 91.28147 | 0.06 |
| 240Pu | 8.46818 | 0.62 |
| 241Pu | 0.17635 | 0.73 |
| 242Pu | 0.0469 | (10) calculated with „new algorithm" |
| 241Am | 0.83514 | 0.38 |

**Containers:**

| | | | |
|---|---|---|---|
| 1. Outside container: | PERLA mod 5 no. A7 | | |
| | gross mass of the container with label: | | 261.4 +- ... g |
| 2. PVC bag: | 1.8 g | | |
| 3. Al capsule: | cylindrical container | | |
| | outside diameter: | 19 mm | |
| | outside length: | 46 mm | |
| | side wall thickness: | 3 mm | |
| | bottom thickness: | 5 mm | (with 2 mm slot for screw driver) |
| | plug thickness: | 8 mm | (with 2 mm slot for screw driver) |
| | Al tightning disk: | 2 mm | |
| | total Al mass: | (23.4 ± 0.2) | |

**Figure 5 Pu sample PM3 at JRC-Ispra.**

The third set of tests used a unique JRC-Ispra resource, a mock-up of a pressurized-water reactor (PWR) fuel assembly. The assembly contains a 17 x 17 grid with 25 guide/instrument tubes and 264 fuel rods. The fuel-rod pitch is 1.257 cm. The cladding outer diameter is 0.968 cm and the inner diameter is 0.854 cm. The fuel pellet diameter in the rods is 0.8123 cm, the $UO_2$ fuel density is 10.46 g $cm^{-3}$, and the fuel loading mass is 1.2615 kg $cm^{-1}$.[2] A schematic layout showing the unique fuel-pin identifications in the JRC-Ispra catalogue is shown in Figure 6. The fuel enrichment was 3.1 %. The length of the fuel region of the assembly was approximately 1.29 m.

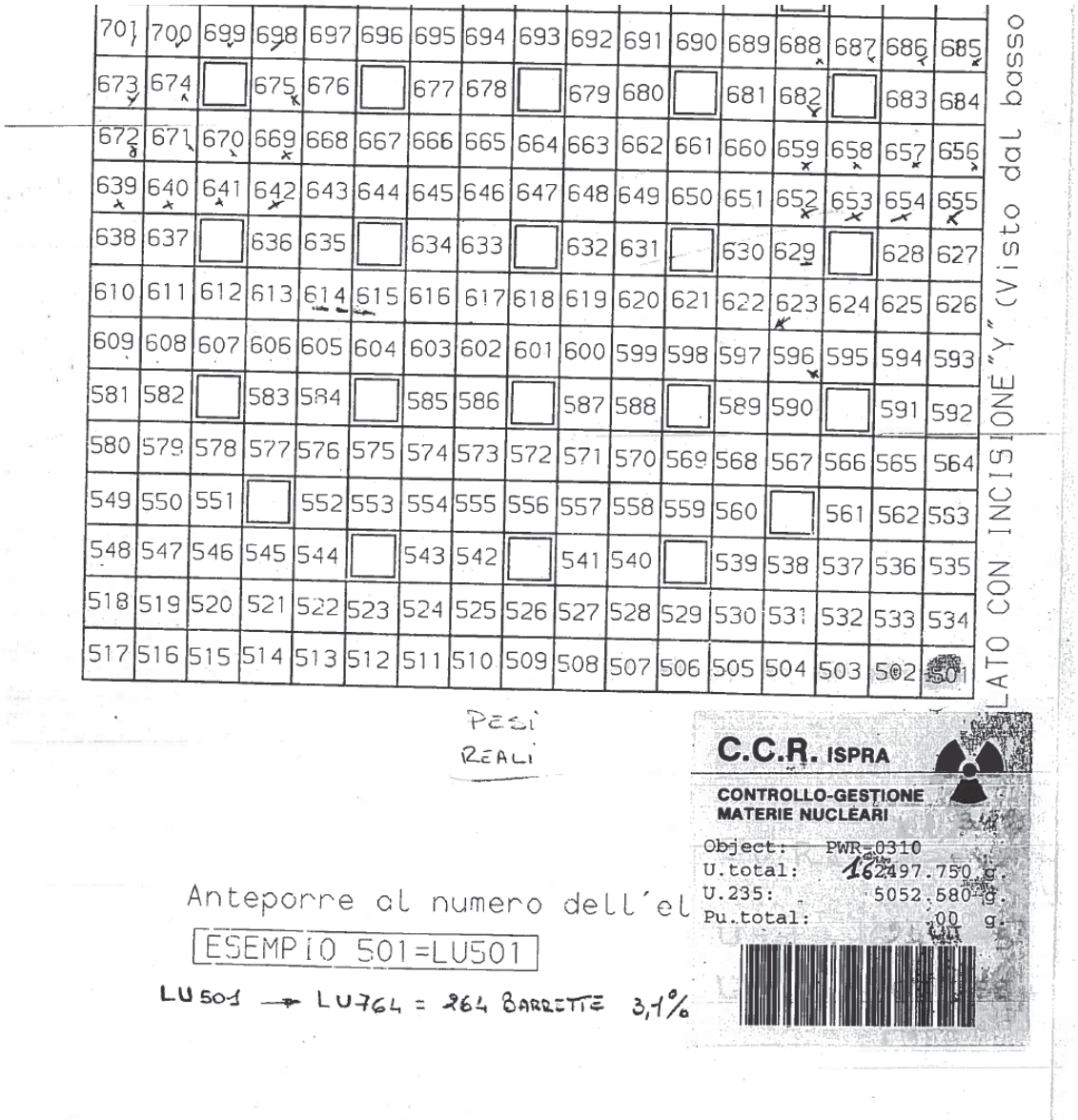


**Figure 6 The fuel-pin ID layout of the PWR LEU assembly.**

## 2.2 Neutron Sources

The AP-ENG used for these experiments was an experimental unit, Model TPA17, manufactured by EADS SODERN (France). Its maximum neutron yield was limited to $10^7$ n $s^{-1}$. Basic principles of AP-type ENGs have been described elsewhere.[3] These devices emit neutrons continuously but are capable of time-tagging a small portion of the emission solid angle by registering alpha particles correlated with discrete deuterium-tritium (DT) fusion events. This registration is performed using a detector that sits inside the ENG neutron tube's vacuum boundary. For the device used for these experiments the alpha sensor was an inorganic scintillator-based detector made of yttrium aluminium perovskite (YAP). The alpha particle from a DT fusion event has an initial speed of 1.3 cm $ns^{-1}$, while the 14.1 MeV neutron has a speed of 5.2 cm $ns^{-1}$. Simple geometry and timing may be used to isolate neutrons in an inverted cone with its apex located at the center on the ENG's beam target (where the DT fusion occurs) by understanding the location of the alpha detector and carefully determining the time-of-arrival of alpha events in this detector. A photograph of the AP-ENG used for these experiments is shown in Figure 7. The ENG was housed in an aluminum-skinned box (towards the left in the figure). In order to determine the spatial orientation of the tagged-beam emanating from the instrument a series of measurements was performed using a liquid scintillator neutron detector and fast-timing electronics. The photograph shows one of these measurements being performed,

**Figure 7 Photograph of one liquid-scintillator detector in position for scanning the tagged-beam region characterizing the AP-ENG.**

In addition to using the AP-ENG, active neutron interrogation measurements were also performed using a $^{241}$Am-Li neutron source. Details of this source have been published elsewhere.[4,5] The neutron yield of the neutron source was approximately 9.4 $\times$ $10^4$ $s^{-1}$; the source contained a small level of beryllium contamination leading to a small higher-energy contamination of the neutron spectrum amounting to approximately 440 $\pm$ 40 $s^{-1}$.

## 2.3 Detectors and Data-Acquisition Instrumentation

The detectors used for these experiments consisted of five EJ-309-based liquid scintillator (LS) detectors. Each detector had a cylindrical sensitive volume that was 13 cm in diameter and 13.3 cm in length. These detectors have been used previously by the collaboration and have been described elsewhere.[6,7] Data acquisition was performed using a CAEN V1720, 8-channel, 12-bit, 250 MHz digitizer. Each channel provided time-synchronized pulse information and was discriminated to only process events corresponding to neutron pulse-events exceeding approximately 600 keV. A separate data acquisition channel was used to record alpha-detection events from the AP-ENG, which used a photomultiplier tube to record scintillation events from alpha particles in the neutron tube. Example plots of the pulse shape discrimination (PSD) performance of these five detectors are shown in Figure 8.

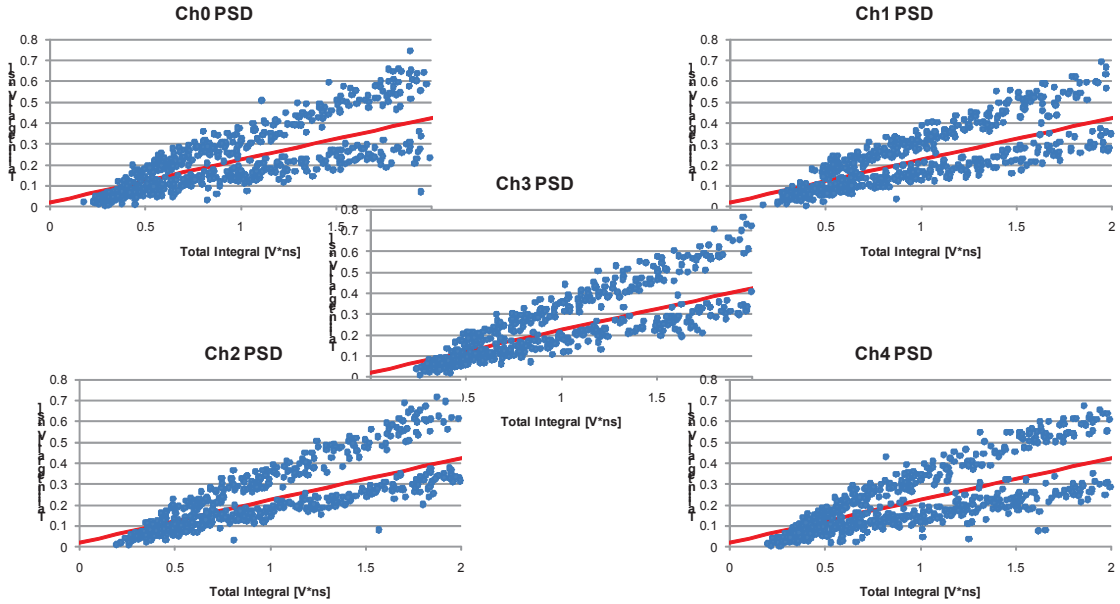


**Figure 8 Example PSD plots of the five LS detectors showing neutron-photon discrimination performance.**

For measurements with the AP-ENG the five LS detectors were mounted to an aluminum support arch which held the detectors suspended over the test area, as shown Figure 9. Detectors 1, 3, and 5 were in a backward-angle (greater than 90 degrees) with

respect to the direction of travel of the tagged DT neutrons, with detector 3 at the largest backward angle, while detectors 2 and 4 were in a forward angle (less than 90 degrees).

For measurements with the Pu disks and the PWR fuel assembly four and three detectors were used, respectively, in a horizontal measurement plane parallel with the floor. Images of these arrangements are included in the sections that follow.

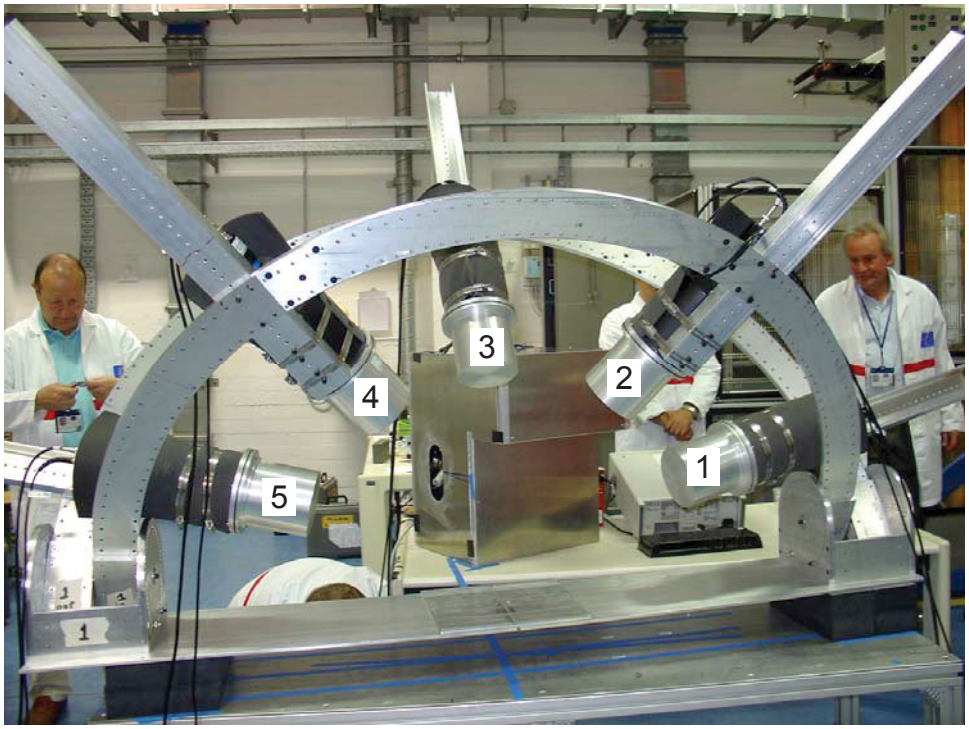


**Figure 9 Photograph of the liquid-scintillator array positioned in front of the AP-ENG for a background measurement.**

## 2.4 Experiments – Uranium Enrichment Standards

Another view of the detector arch used for the uranium enrichment standard measurements is shown in Figure 10. The AP-ENG is to the left of, and behind, the detector arch. Also shown in this figure is a polyethylene platform that was used to elevate the uranium containers and provide a source of neutron moderation when using the AmLi source. For each uranium enrichment standard both an AP-ENG interrogation and an AmLi interrogation was performed. A close-up photograph of the AmLi source inside the moderate is shown in Figure 11. A photograph of a uranium enrichment canister in position for measurements is shown in Figure 12.

**Figure 10 Photograph of the AmLi source positioned within the polyethylene assembly in the detector arch, for collecting the background spectrum.**

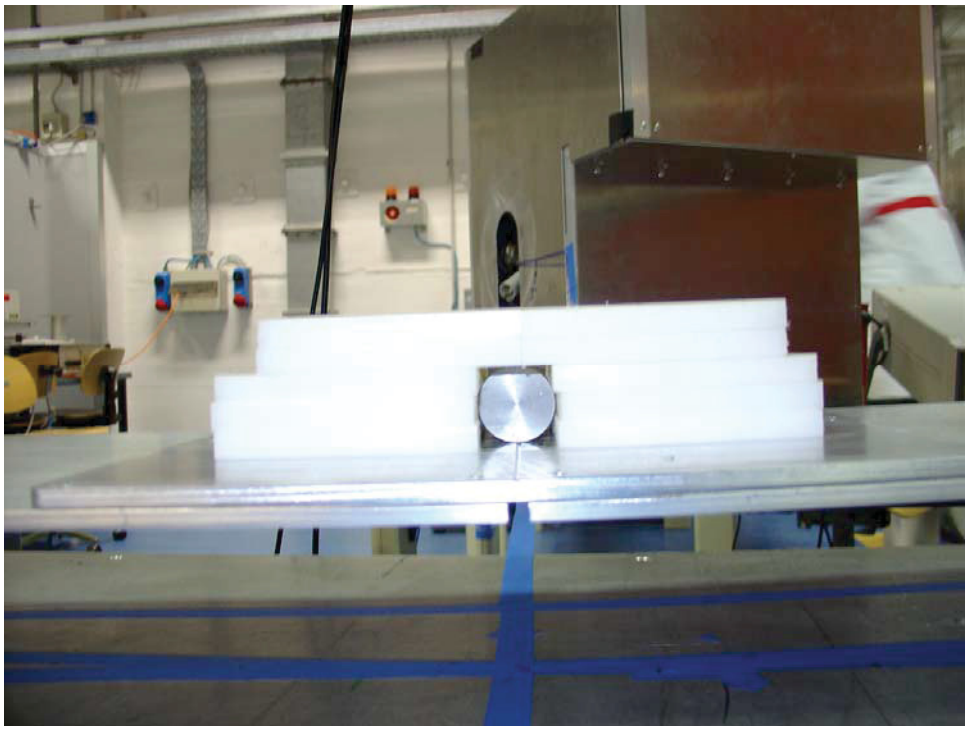

**Figure 11 Close-up photograph of the AmLi source in the configuration used for irradiating the uranium oxide fuel.**

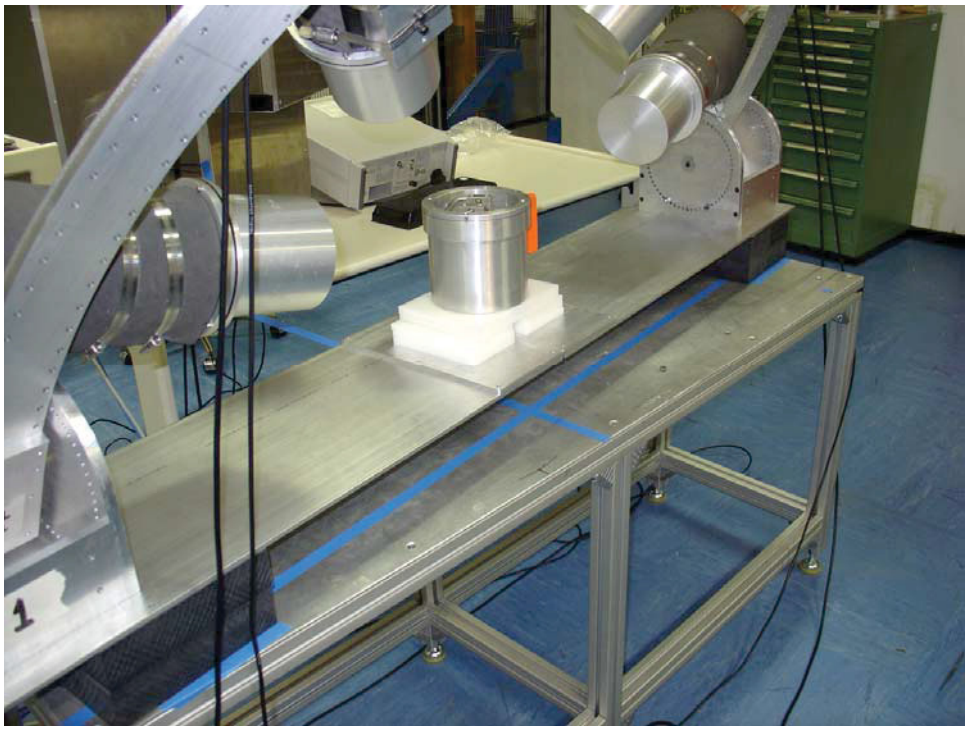

**Figure 12 The uranium oxide fuel in position for irradiation under the detector arch.**

## 2.5 Experiments – Passive Pu Assay

A photograph of the four detectors in position to measure the three Pu disks is shown in Figure 13. A side view of this same arrangement is shown in Figure 14.

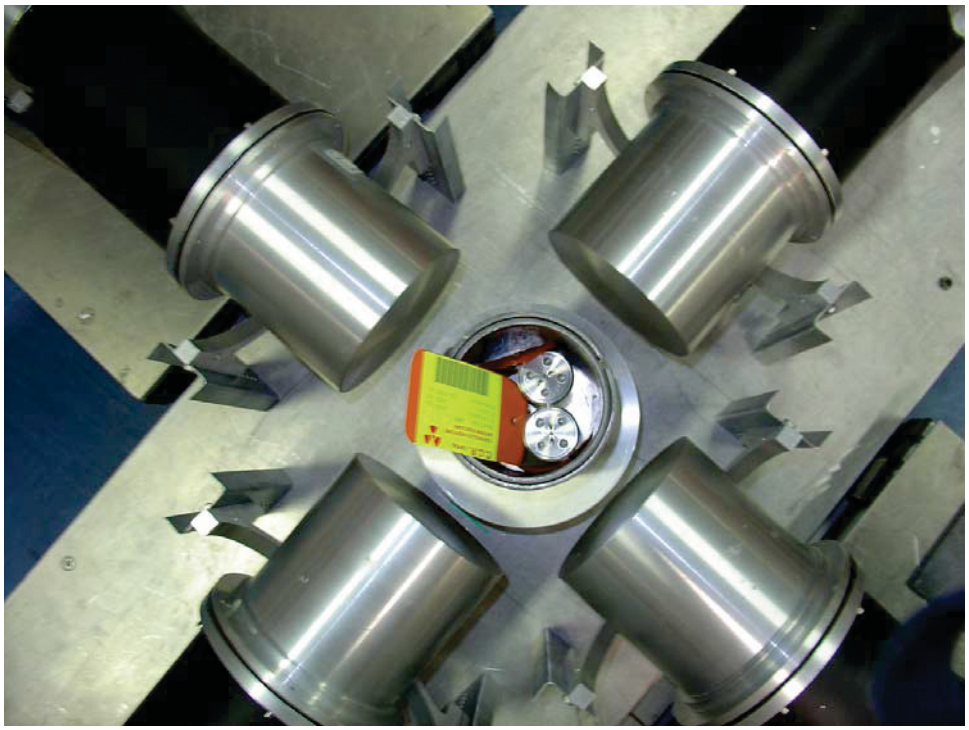

**Figure 13 Top-view photograph of the three plutonium samples, within a lead sleeve, centered between the four liquid-scintillator detectors,**

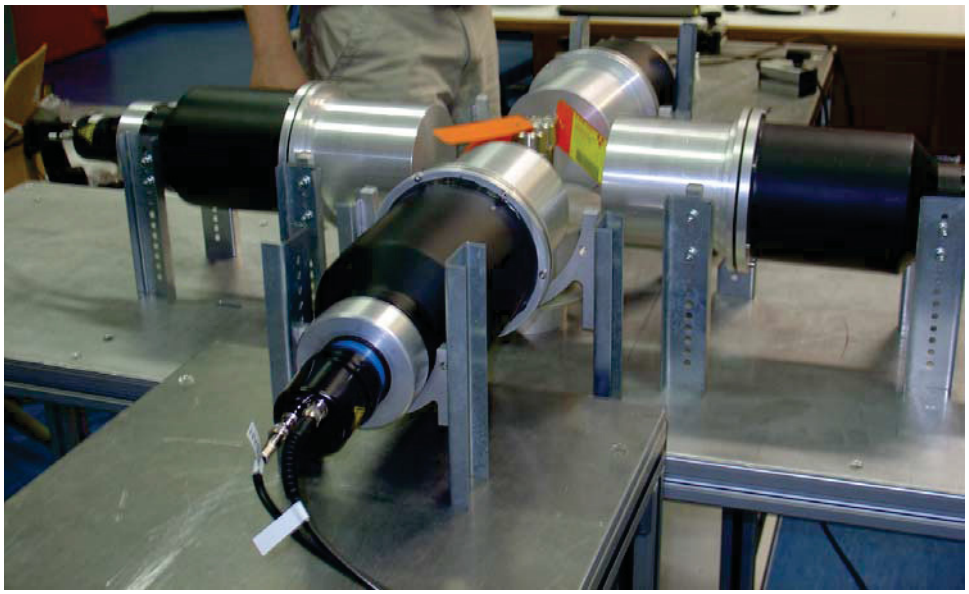

**Figure 14 Side-view photograph of the three plutonium samples, within a lead sleeve, centered between the four liquid-scintillator detectors.**

## 2.6 Experiments – PWR Fuel Assembly

A photograph of the three LS detectors being arranged next to the PWR fuel assembly is shown in Figure 15. To the left of the assembly a polyethylene cylinder is being positioned along one side of the assembly. This cylinder contained an inner lead

sleeve; the dual-cylinder arrangement was used to hold the AmLi source for active interrogation measurements of the PWR assembly, shield the detectors from gamma rays from $^{241}$Am in the AmLi source, and provide a modest level of premoderation to the AmLi neutrons. A close-up photograph of this arrangement is shown in Figure 16.

**Figure 15 Photograph showing the detectors being aranged on three sides of the PWR fuel assembly, with cylindrical polyethylene and lead sleeves being positioned to receive the AmLi source.**

**Figure 16 Close-up photo of the AmLi source in the cylindrical sleeves of polyethylene and lead.**

# 3 Preliminary Analysis – Experiments and Modeling

The JRC-Ispra experiments described in this report took two weeks. Data analysis and interpretation will take considerable longer. Indeed, Section 4 of this report includes new data analysis the collaboration took in 2009. This section provides a snap-shot of the preliminary analyses performed during the summer of 2011. This analysis is focused almost exclusively of the AP-ENG active neutron interrogations of the three uranium enrichment standards. Further work will be needed to continue parsing through the different data sets and interpreting the measured results in consultation with new simulations that will need to be performed.

## 3.1 The Model Geometry

A schematic representation of the MCNP-PoliMi model used to model the detectors and the uranium enrichment cylinders is shown in Figure 17. Comparing this rendering with Figure 10 several simplifications are evident including the lack of the arch, the lack of floor, walls, and ceiling, and the lack of the ENG housing. New iterations of this model are underway to continue adding experimental details and increase the model's fidelity but, at the close of FY2011, these additions were not yet available for inclusion in this report. This model geometry is the basis for results presented in this section of the report.

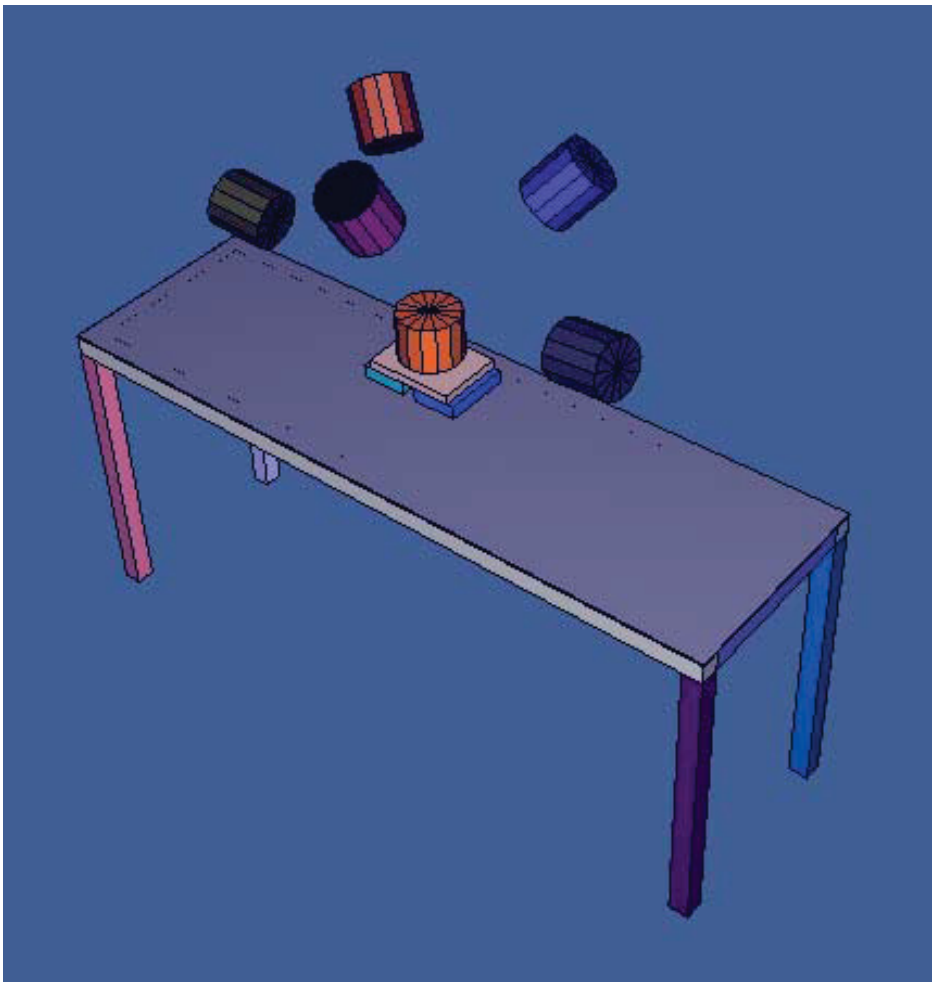

**Figure 17 Screen-shot rendering of the solid-geometry model used to represent the AP-ENG interrogation in the MCNP-PoliMi code.**

## 3.2 Preliminary Simulation TOF Results

The simulated neutron time-of-flight (TOF) response of the five detectors for irradiation of LU 44 is shown in Figure 18. LS detectors 1, 3, and 5 have less obvious TOF contributions from the scattered 14-MeV neutron peaks: these three detectors require a greater scatter angle and therefore more neutron energy loss before detection. LS detectors 2 and 4 have a more significant 14-MeV scatter peak. Exploring this further, a separate set of simulations was performed using MCNP5 and a post-processing data analysis tool that extracted the time-correlated event histories from the MCNP5 PTRAC data output. These results are presented in Figure 19. In this figure the individual reactions that lead to the separate response profiles shown in Figure 18 have been explicitly plotted.

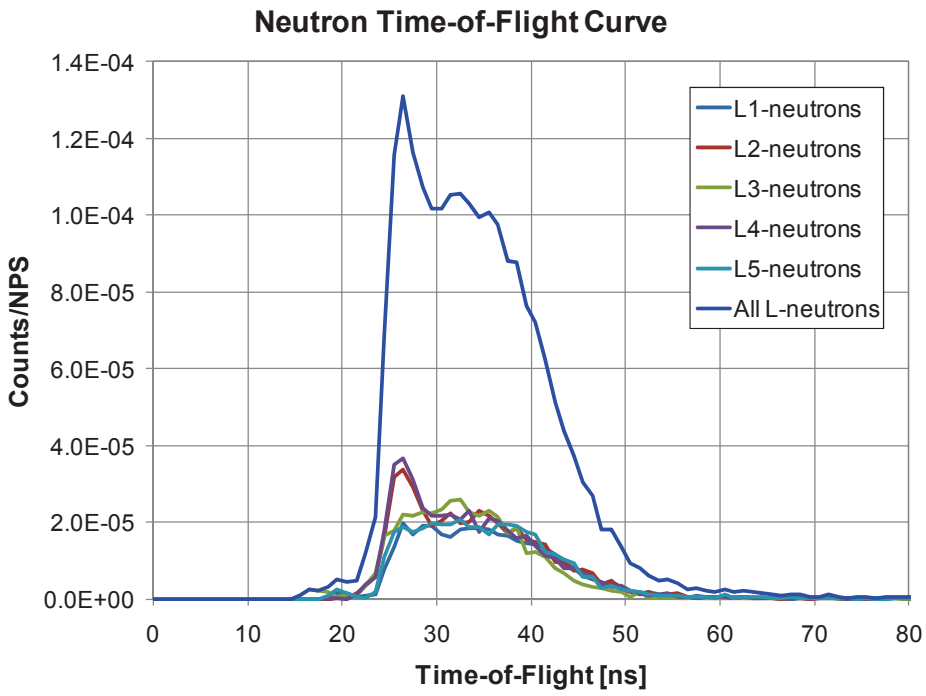


**Figure 18 MCNP-PoliMi simulated neutron TOF responses.**

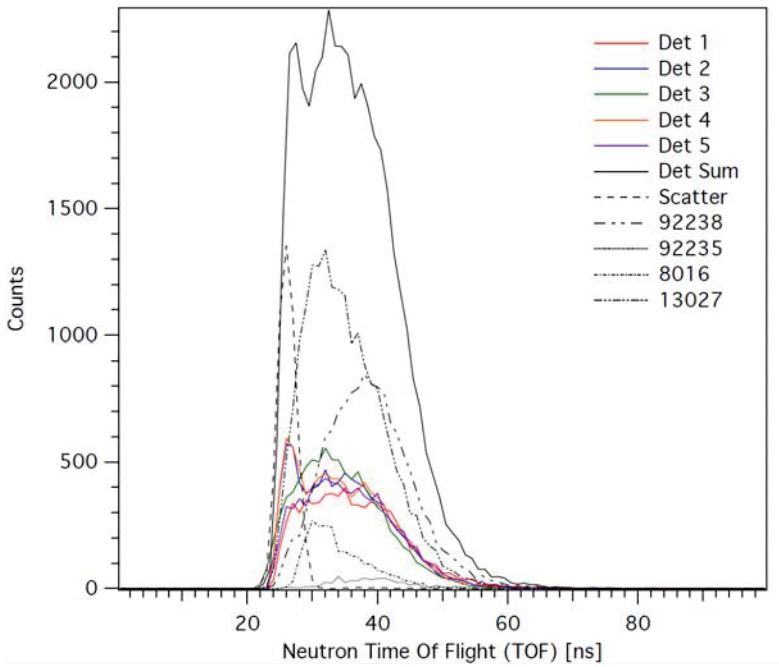


**Figure 19 Simulation of the AP-ENG induced TOF spectrum for irradiation of the 3%-enrichment uranium sample measured with the five liquid scintillators, including a breakdown of the reaction components leading to the signal (calculated using MCNP5).**

Reviewing Figure 19 it is clear that, as expected, the initial spike in the TOF corresponds to scattered neutrons. Arriving earliest in time, these are also the highest energy neutrons in the system in the time period following the arrival of the DT fusion neutrons. Later in time, the contribution to the TOF spectrum from (n,Xn) reactions with oxygen and aluminum are evident. So too is the (n,fission) prompt neutron contribution from $^{238}$U (intense) and $^{235}$U (weak).

A comparison of the total detector array (all five detectors) response for the three uranium items is shown in Figure 20, the green trace for LU25 is not visible beneath the blue trace for LU44. The primary difference between these corresponds to the total uranium mass.

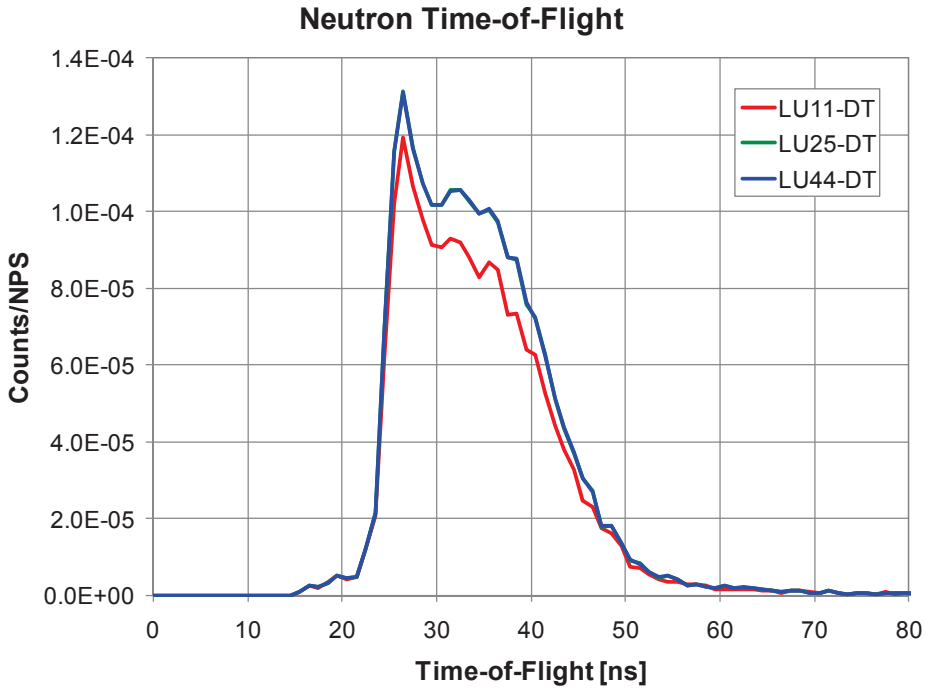


**Figure 20 MCNP-PoliMi simulated TOF response for each fo the three uranium standards.**

## 3.3 Observed Pulse Height Responses

Representative pulse-height responses measured for the five LS detectors are presented in Figure 21. For this figure detector events correspond to the presence of tagged DT neutrons in the inspection region, as determined by using the AP-ENG alpha sensor. Detectors 2 and 4 show a strong 14.1 scattered-neutron component, which is only possible for these two detectors, and not detectors 1, 3, and 5, since they are at large scattering angles. Detectors 1 and 5 show a fast-neutron peak corresponding to a slightly degraded energy, due to the higher scattering angle for (n,n') neutrons to reach these.

Detector 3, which is at an even larger scattering angle (with respect to the incident tagged neutron beam) than detectors 1 and 5, shows the largest energy loss.

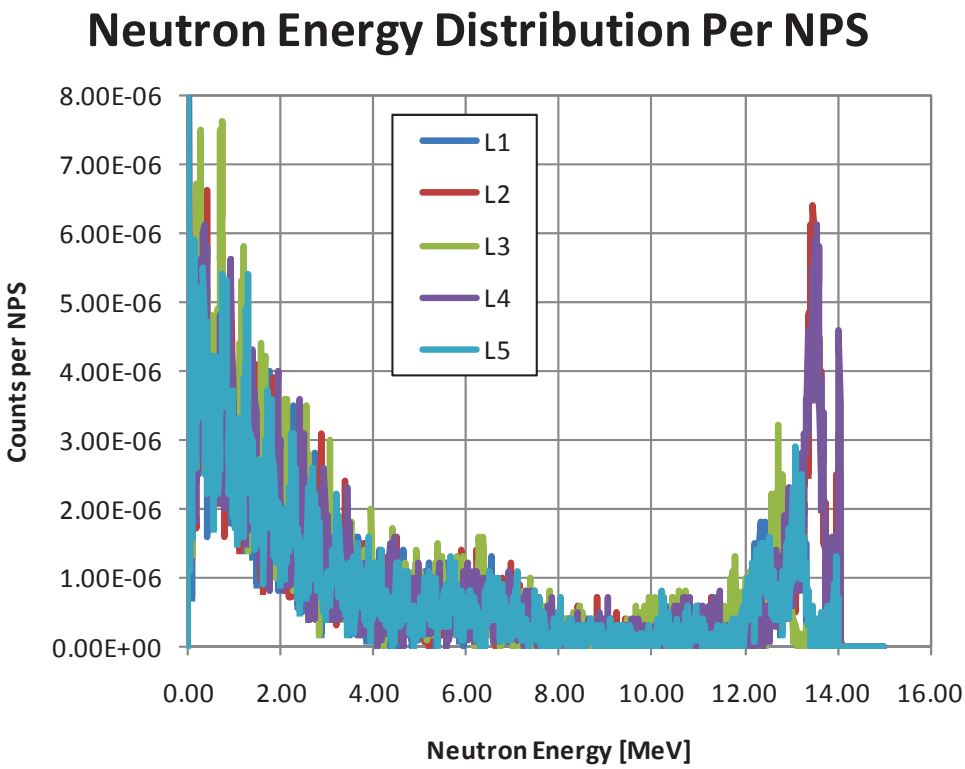


**Figure 21 Representative pulse height distributions for the five detectors.**

## 3.4 Observed TOF Spectra

The measured TOF spectra for each of the three uranium enrichment standards is shown in Figure 22. The data shown here has been shifted in time to approximately center the DT neutron scatter peak at time t = 0 ns. The prominent inelastic scattering peak is clearly visible; the photon response is not shown. The inelastic scatter peaks for the three cases appear broader than might be expected due to the slight time-of-arrival difference for the five detectors, the signals from which have been added together in each case. To allow for a clearer comparison of the (n,Xn) and (n,fission) regions of the total TOF spectra, the response of each of the five detectors has been individually trimmed to eliminate the scattering peaks, and then added together for each of the three cases. This modification is shown in Figure 23. The total intensity in this time region is smallest for LU11, the low-mass, low-enrichment standard. The equal-mass standards LU25 and LU44 show comparable total amplitudes but the integral for LU25, which contains slightly more $^{238}$U than LU44 is slightly more intense. Over the course of the measurements the neutron yield from the ENG was not constant; this has not yet been accounted for in this data. The fast-fission neutron yield from $^{235}$U at 14 MeV is 1.8X that for $^{238}$U, as shown in Figure 24. It is feasible that for higher levels of enrichment the

relative intensity of the inelastic scatter peak in comparison with the (n,Xn) and (n,fission) region may provide an indication for determining enrichment. For these studies, however, the difference is low and follow-on experiments with the AmLi source were explored as a method for identifying the $^{235}U$ components of the mixtures.

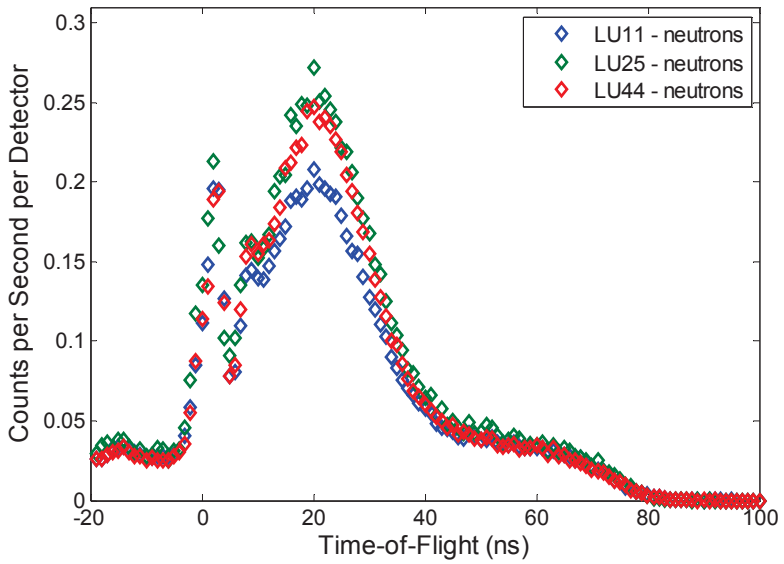


**Figure 22 Measured TOF neutron spectra (all five detectors summed together) for each of the three uranium samples.**

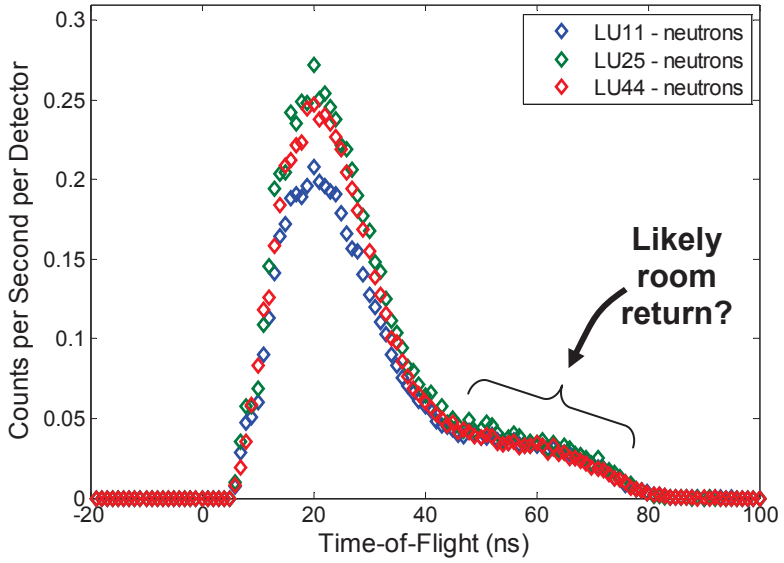


**Figure 23 Measured TOF neutron spectra (all five detectors summed together) for each of the three uranium samples, with each detector's contribution to each spectra individually trimmed to eliminate the neutron scattering components.**

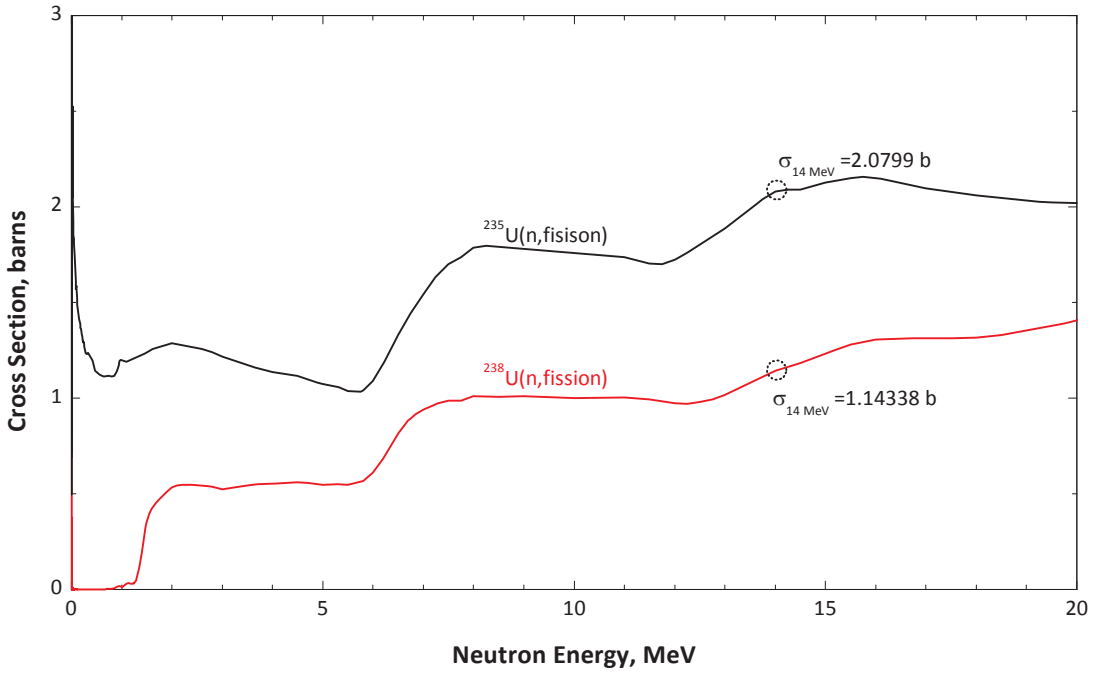


**Figure 24 Fast-fission cross sections for $^{235}$U and $^{238}$U.**

## 3.5 Preliminary Comparison of Simulations and Experiments

A comparison of the total simulated photon and neutron TOF response with the observed response (all five detectors) is shown in Figure 25. The simulated response has been adjusted to account for the threshold settings used with the LS detectors in the measurements. The general shape of the photon response is in excellent agreement, which is expected since this signature is independent of deviations between the simulation and the measurements in terms of photon energies. The magnitudes of the measured responses are slightly less than for the simulation, which may be due to an incorrect assumption for the ENG yield. Further analysis of the measured alpha-particle signal rate will be needed to account for this. Also, detector-to-detector scattering has not yet been included in the simulations.

The profiles of the neutron TOF spectra in the two plots also show generally good agreement. One clearly seen difference between the two plots is the nearly constant offset in both photon and neutron signals that under lays the TOF responses from 0 ns to about 70 ns. At this time this is thought to be due to the lack of inclusion of the floor, walls, and ceiling in the simulations. Future work will be performed to examine these features.

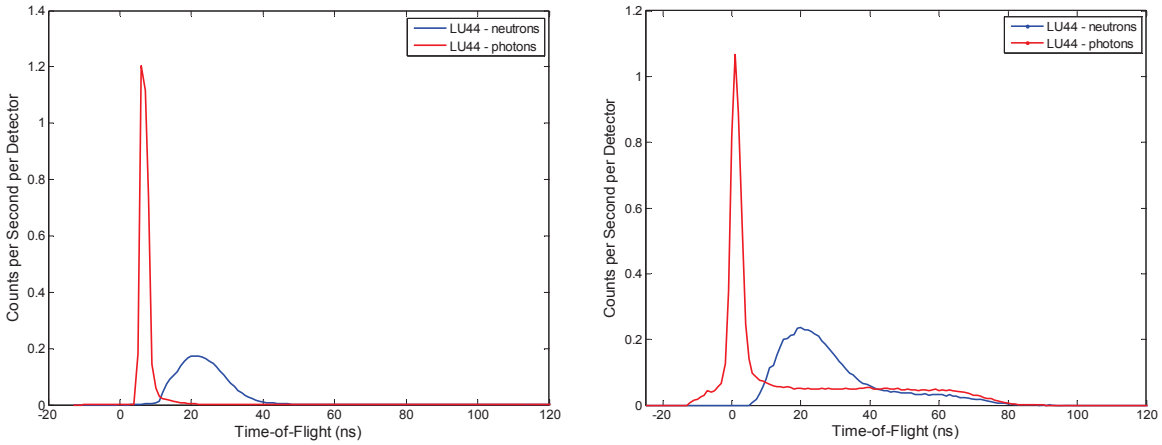


**Figure 25 Simulated (left) and measured (right) photon and neutron TOF spectra for LU44 (note the different scales).**

## 3.6 Preliminary Observations and Conclusions

- Inelastic scattering of the fast DT neutrons is evident in the TOF spectrum at the earliest time intervals; the scattered neutron intensity is different in the different detectors as a function of scattering angle. (The double-differential (n,n') scattering cross sections for $^{235}$U and $^{238}$U are shown in Figure 26.) Relative changes versus scattering angle are comparable for both $^{235}$U and $^{238}$U, which precludes enrichment determination based on scattering angle alone. However, the angular scattering cross-sections for uranium are different than for oxygen, which may permit separating the uranium and oxygen components if needed.

**Figure 26 Double differential (n,n') scattering cross sections for $^{235}$U and $^{238}$U.**

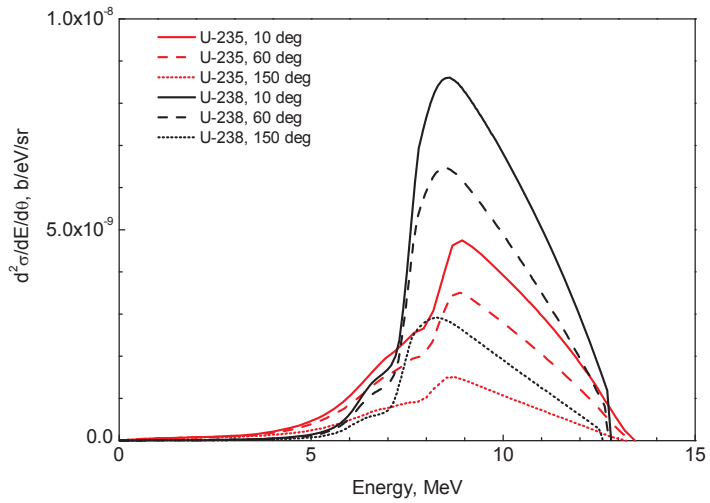


- At later times in the TOF spectrum the prompt-fission contribution from U is important but the contribution of inert matrix materials cannot be ignored.

- Examining the fission-region of the DT TOF spectrum provides a measure of total uranium, while the AmLi measurements will help to quantify the fissile fraction. (The analysis of this data is still to be done.)
  - This approach shares similarities with the use of an active well counter, with added information about total uranium.
  - This approach may be suitable for unusual geometries, or poorly defined/characterized geometry.
  - Potential for determining uranium enrichment as well as total mass.
  - Capable of penetrating through shields.
  - Potentially a low infrastructure measurement, could allow assay inside storage containers.
  - It may be possible to mimic the effects from using an AmLi source by switching operation of the ENG from continuous mode (for AP measurements) to a pulsed mode, for die-away analyses.
- TOF spectrum deconvolution, as hinted at in Figure 19, holds promise for further data mining (isotopic differences for (n,n'), (n,2n), (n,3n), and fission-neutron energies).
- Time correlation with prompt gamma-ray neutron spectrometry may provide independent $^{16}O$ determination.
  - Differences in forward vs. backward elastic scattering.
  - Similar possibilities in fluorine may support extension to $UF^6$ enrichment assay.
- DT irradiation coupled with thermal neutron detection (vs. liquid scintillators) may eliminate need for AmLi, in die-away time region, when using a pulsed ENG.
- The limited detector coverage of this experiment precluded adequate collection of neutron data adequate for higher-order coincidence analysis.

# 4 Anisotropy Analysis

Recently published work has suggested an approach for fast-neutron measurements where the inherent anisotropy of correlated fission neutrons might be used as an additional component for safeguards assay measurements.[8,9] Approximately 10% of the prompt neutron produced during a fission event are released during the scission of the parent nucleus, the remaining 90% of the prompt neutrons are produced in the immediate decay of the fission products isotopes. A fraction of these neutron emissions occur while the fission product atoms are still in motion, with kinetic energy from the fission itself. Anisotropy in the observed prompt-fission neutron distribution is a result of the movement of these fission products. While neutron emission from these atoms will be isotropic in their moving coordinate systems, in the laboratory frame of reference these emissions are biased in the direction of travel of the fission products. A

moderate bias has been reported in experimental observations analyzed by Holewa and Charlton.[8]

In neutron coincidence measurements it is important to be able to account for the fraction of uncorrelated neutrons originating from ($\alpha$,n) reactions versus correlated neutrons (fission neutrons) in the gross neutron count rate. Uncorrelated neutrons from ($\alpha$,n) reactions do not contribute to anisotropy measurements while fission neutrons do. For well characterized measurement conditions, a measure of neutron-pair anisotropy using fast liquid scintillators may allow for differentiating the ($\alpha$,n) component from the total neutron rate of an assembly of SNM. Observed fission anisotropy may also provide insight related to material form, porosity, and density (fission-fragment range in mater). As a first step towards exploring this, we have chosen to re-analyze data from our 2009 experiments at INL, as well as our recent JRC-Ispra experimental data, to examine this signature.

## 4.1 2009 Anisotropy Data from ZPPR

In 2009 the INL-University of Michigan collaboration performed passive fast-neutron correlation measurements with MOX fuel pins at the INL ZPPR facility. In one case 90 pins (15.24 cm in length) of low $^{240}$Pu-content fuel was used while in the other case 90 pins of high $^{240}$Pu content fuel was used. Details for these materials and the experiments have been published previously.[10] Four detectors were used, all parallel to the floor, at angles of 0°, 90°, 180°, and 270°. Plots of the side-by-side detector correlations (90 degree pairs) and opposite detector correlations (180 degree pairs) for each type of fuel pin are shown in Figure 27. The ratio of 180 degree (nominal correlated) to 90 degree (nominal uncorrelated) neutron emissions was 1.25 and 1.31 for the low and high $^{240}$Pu cases, respectively. Using MCNP-PoliMi to evaluate the neutron source term for these two MOX fuel materials, a comparison has been made of the fission source term to the ($\alpha$,n) source term intensity in each can. The source term ratios for the two cans were 1.27 and 1.59, respectively. It seems clear that anisotropy has been observed for the two cans with a trend that correctly follows the ration of fission to ($\alpha$,n) neutron rates for the two cans.

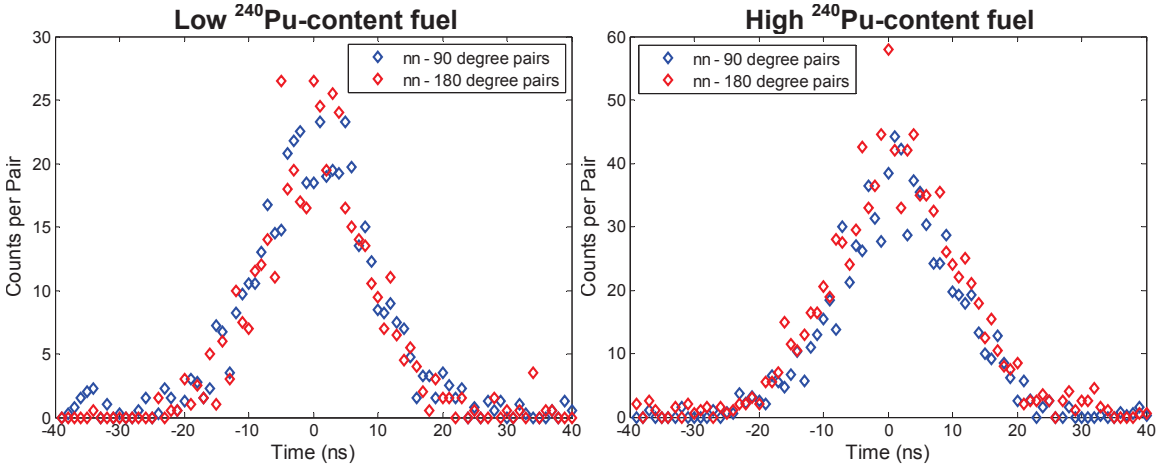


**Figure 27 Angular neutron correlations at 90 degrees and 180 degrees for low $^{240}$Pu content and high $^{240}$Pu content MOX fuel pins.**

Measurement of neutron anisotropy was not an objective of these previous experiments. It would be questionable to extract more meaning from the above data beyond the observed presence of anisotropy. However, the simple nature of the measurement, and the value such measurements may provide to augment LS-based, fast-neutron time-correlation studies in further safeguards instrumentation research and development, suggests this is a topic worthy of future study.

## 4.2 2011 Anisotropy Data from JRC-Ispra

Analysis has also been performed to analyze recent data collected of the three plutonium disks while at JRC-Ispra. The raw neutron and photon time-correlation plots from the measurement geometry of Figure 13 and Figure 14 in are shown Figure 28. The n-n coincidence components of these are shown on top of each other in Figure 29. The observed ratio of 180 degree/90 degree correlations was 1.14. Considering the plutonium for these measurements was in metallic form, and not an oxide, a much higher 180:90 signal ratio would be expected. Unfortunately, as seen in the photographs of the experiment, the four detectors were very close together for these observations. Prior MNCP-PoliMi modeling has shown the deleterious impact such close spacing can have for time-correlation studies. While simulations for this measurement configuration have not yet been performed, it seems likely that cross-talk between the detectors may have been significant. Also, since the detectors were very close together, the TOF resolution for these measurements was also not large. This too may have served to diminish the observed anisotropy.

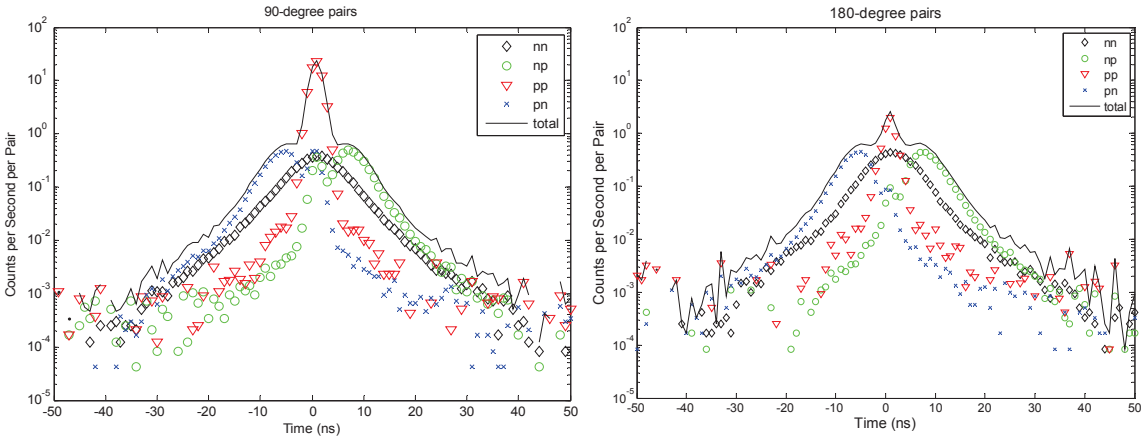


**Figure 28 Neutron and photon correlation measurements at 90 degrees and 180 degrees from JRC-Ispra using three plutonium metal samples.**

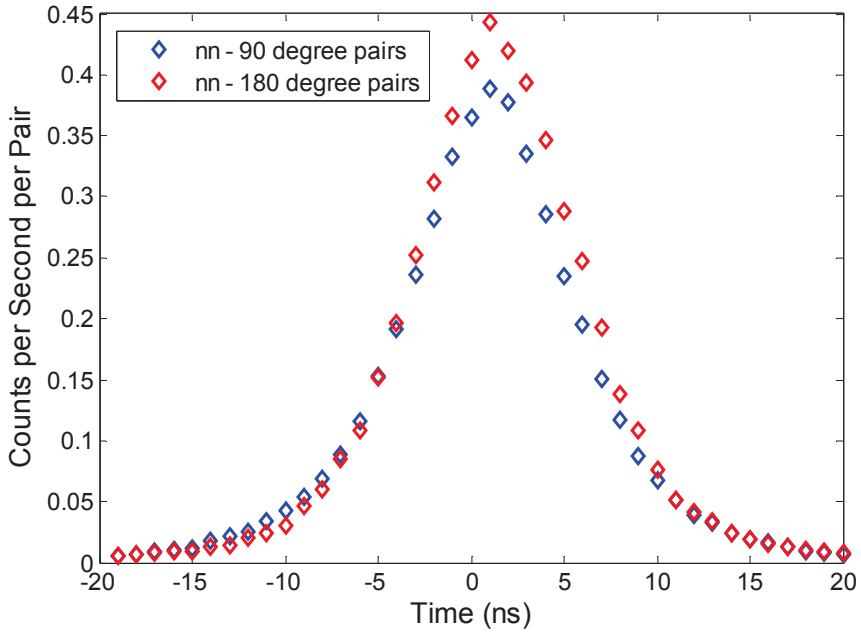


**Figure 29 Comparison of 90 degree and 180 degree neutron correlations observed at JRC-Ispra.**

# 5 SUPPORT FOR THE ORNL RADIAL-IMAGER PROJECT

In addition to the work described above, in FY2011 INL provided support to Dr. Paul Hausladen of Oak Ridge National Laboratory and his research team. In FY2011 ORNL had a project to develop and test a novel fast-neutron imaging system designed to scan an assembly of neutron-emitting fuel rods. The purpose of this system was to demonstrate the feasibility of using neutron-based imaging system for detecting and locating the removal of a single-pin fuel pin in a mixed-oxide fuel assembly. (Details of

this system and preliminary results of the measurements will be presented in a subsequent ORNL report.) INL's support to ORNL involved a) working with Dr. Hausladen to design a suitable test fixture for the experiments, b) assembling test fixtures containing plutonium-uranium fuel pins, and c) hosting the ORNL team for an experimental campaign. The experiments took place at INL's Materials and Fuels Complex (MFC), and the ZPPR facility (formerly the zero-power physics reactor).

## 5.1 Test Fixture Design

Considering the expected measurement capabilities of the ORNL prototype measurement system, and INL's capabilities and limitations for handling special nuclear material, early discussions focused the design effort towards a fixture concept holding 32 ZPPR-style fuel pins in a semi-square array. Idaho National Laboratory possess a diverse variety of special nuclear materials useful for validating passive screening and active interrogation nondestructive analysis techniques for nuclear safeguards and MPC&A.[11,12] A review of INL's material inventory identified the 15.24-cm (6-inch) long PUOH (Identification number (ID No. 129) mixed-oxide (MOX) fuel as the ideal candidate for these tests. It contains both plutonium and uranium and is held in a steel cladding. This material is representative of plutonium recycled from high burn-up spent fuel (26% $^{240}$Pu), which is postulated for use in advanced fuel cycle concepts under development in the Fuel Cycle Research and Development program. In addition, INL possesses a set of depleted-uranium (DU) fuel pins (UODR, ID No. 130) of nearly identical mass as the PUOH family of pins, making them an ideal surrogate to use for testing the ORNL system's ability to detect and locate a missing pin. A summary of the composition of these two fuel pin types is shown in Table 1. Plans were also made to create stainless steel (304SS) pins for use in the imaging studies as well.

Prior work supported through the MPACT program has been carried out to characterize the neutron emission source of the PUOH material.[10] An age-corrected estimate of the neutron source term for this material is given in Figure 30. An MCNP-PoliMi-calculated estimate of the spectrum of the neutron source term for an assembly of PUOH material is shown in Figure 31. The single largest component contributing to neutron emission from this material is the $^{240}$Pu spontaneous fission source term. Neutrons originating from the alpha-decay of the plutonium isotopes, and the subsequent creation of neutrons due to interactions with oxygen in the fuel, amount to approximately one-quarter of all neutron emissions in this material.

**Table 1 The MOX and DU fuel element materials studied in this project (original assay date July 1, 1983). [12]**

| ID No. | 129 | 130 |
|---|---|---|
| Size | 0.9525 cm Ø × 15.24 cm long | 0.9525 cm Ø × 7.62 cm long |
| Average weight | 102.6026 | 102.941 |
| Core weight | 89.7760 | 89.787 |
| Pu weight | 14.0147 | NA |
| $^{238}$Pu | 0.0096 | NA |
| $^{239}$Pu | 9.8079 | NA |
| $^{240}$Pu | 3.6603 | NA |
| $^{241}$Pu | 0.5170 | NA |
| $^{242}$Pu | 0.0200 | NA |
| $^{241}$Am | 0.1473 | NA |
| U weight | 64.5849 | 79.107 |
| $^{235}$U | 0.1391 | 0.159 |
| $^{238}$U | 64.4458 | 78.948 |
| O weight | 10.5936 | 10.642 |
| Clad weight | 12.39 | 12.393 |
| 69.53 wt% Fe | 8.615 | 8.617 |
| 18.54 wt% Cr | 2.297 | 2.298 |
| 9.65 wt% Ni | 1.196 | 1.196 |
| 1.28 wt% Mn | 0.159 | 0.159 |
| 0.47 wt% Si | 0.058 | 0.058 |
| 0.09 wt% Co | 0.011 | 0.011 |
| 0.06 wt% Mo | 0.007 | 0.007 |
| 0.06 wt% Cu | 0.007 | 0.007 |
| 0.05 wt% Ti | 0.006 | 0.006 |
| 0.035 wt% Al | 0.004 | 0.002 |
| 0.028 wt% C | 0.003 | 0.002 |
| 0.02 wt% Ta | 0.002 | 0.001 |
| 0.014 wt% P | 0.002 | 0.001 |
| 0.01 wt% Be | 0.001 | 0.001 |
| 0.007 wt% S | 0.001 | 0.001 |

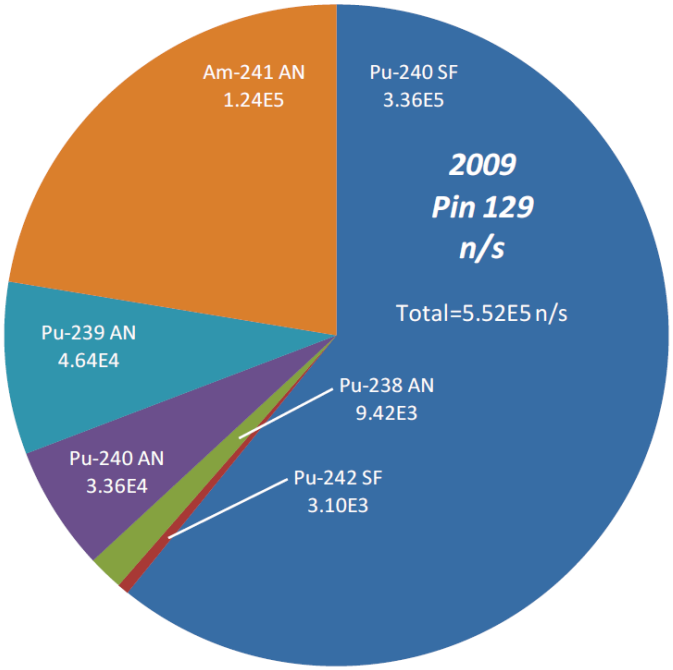


**Figure 30 Neutron emission characteristics of PUOH (ID No. 129) MOX fuel at INL (note: the composition has been corrected for age from the original assay listed above).**

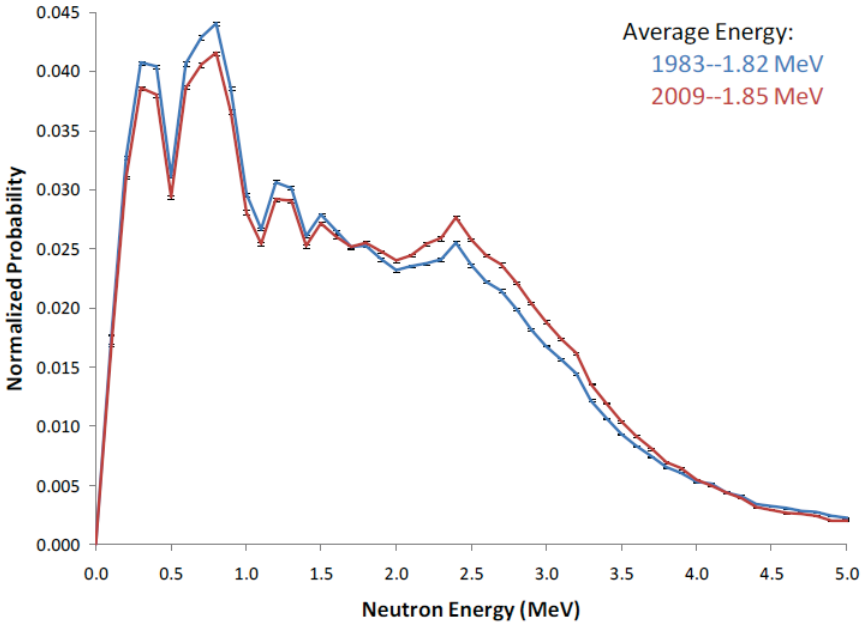


**Figure 31 Estimated fast-neutron spectrum for an assembly of PUOH MOX fuel pins.**

The test fixture developed for this project consisted of two 1.27-cm (0.5-inch) thick aluminum support plates separated by four 13.97-cm (5.5-inch) aluminum rods, each with a diameter of 0.635 cm (0.25 inch).. Each plate, top and bottom, had 32

through holes just slight larger in diameter than the fuel pins. The layout consisted of a square 4 x 4 array with each outer row having an extra four holes in line with the array (4 x 4 +4 x 4 = 32). Thus, the final hole pattern was a 6 x 6 array with the corner holes missing (6 x 6 – 4 = 32). A schematic representation of the hole pattern is shown in Figure 32.

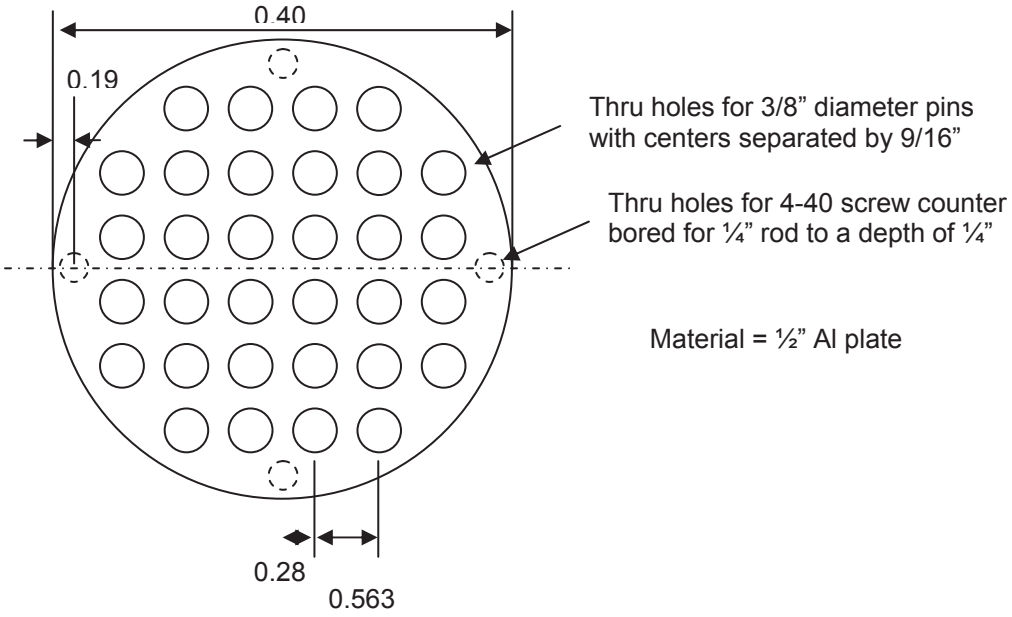


**Figure 32 Schematic layout of the hole pattern in the support plates.**

For use in ZPPR these test fixtures were designed to fit within a stainless-steel can, which acted as a secondary containment for safety considerations. To facilitate loading of the cans, the support plates were designed to have thin top and bottom cover plates that could be attached with screws, thus keeping all of the fuel pins in a confined position to eliminate rattling in the can. The head space above the upper cover plate, when loaded into a can, was approximately 1 cm; this volume was designed to be filled with crumpled aluminum foil, to ensure each fuel pin assembly remained stationary in each can. To further ensure the assemblies do not shift while in storage or during handling, a thin support plate was glued into the bottom of each can that acted as a key to capture the four small screw-caps from the screws used to lock the lower cover plate to the lower support plate. A schematic cut-away drawing of one of these assemblies is shown in Figure 33.

**Figure 33 Schematic cut-away drawing of the support plate assembly and test fixture.**

## 5.2 Test Fixture Assembly

Five test fixtures were manufactured and assembled. One was intended for use in prototype testing, without MOX fuel, while the other four were for use in the experiment with fuel. Four separate loading schemes were developed for the tests, identified as Inspection Object (IO) #1, IO #2, IO #3, and IO #4. To avoid confusion with other inspection objects at ZPPR, the items were also referred to as Can #1, Can #2, etc. A schematic representation of the four pin loadings is presented in Figure 34. A total of 121 MOX pins were used; the total mass of plutonium assembled for these experiments was 1.69 kg.

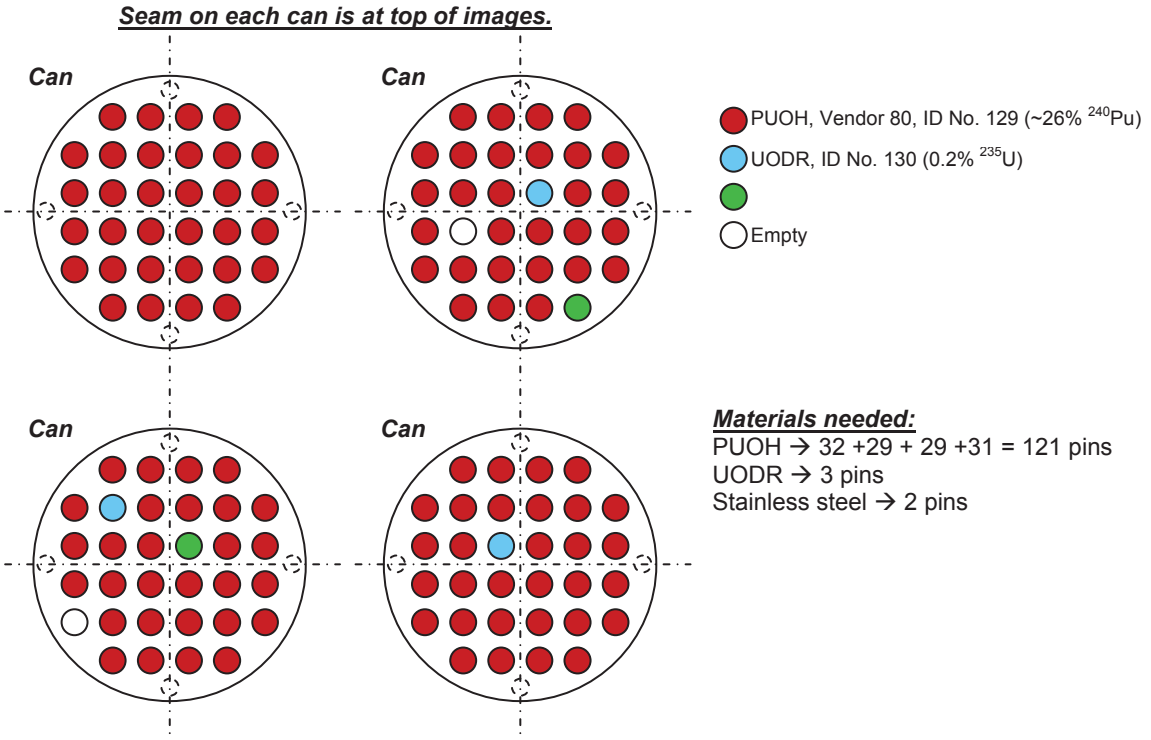


**Figure 34 Layout of MOX fuel pins, DU fuel pins, and steel pins in the four inspection objects.**

Photographs were taken during the assembly process for creating the four inspection objects. Photographs of the four cans, prior to final placement of the top covers and crumpled aluminum foil, and prior to application of the lids to each can, are shown in Figure 35. As an aid during assembly, marks were made to identity the locations for the DU pins and where voids were needed. The steel pins are also clearly visible. A photograph of IO #1 showing the crumpled aluminum foil is seen in Figure 36.

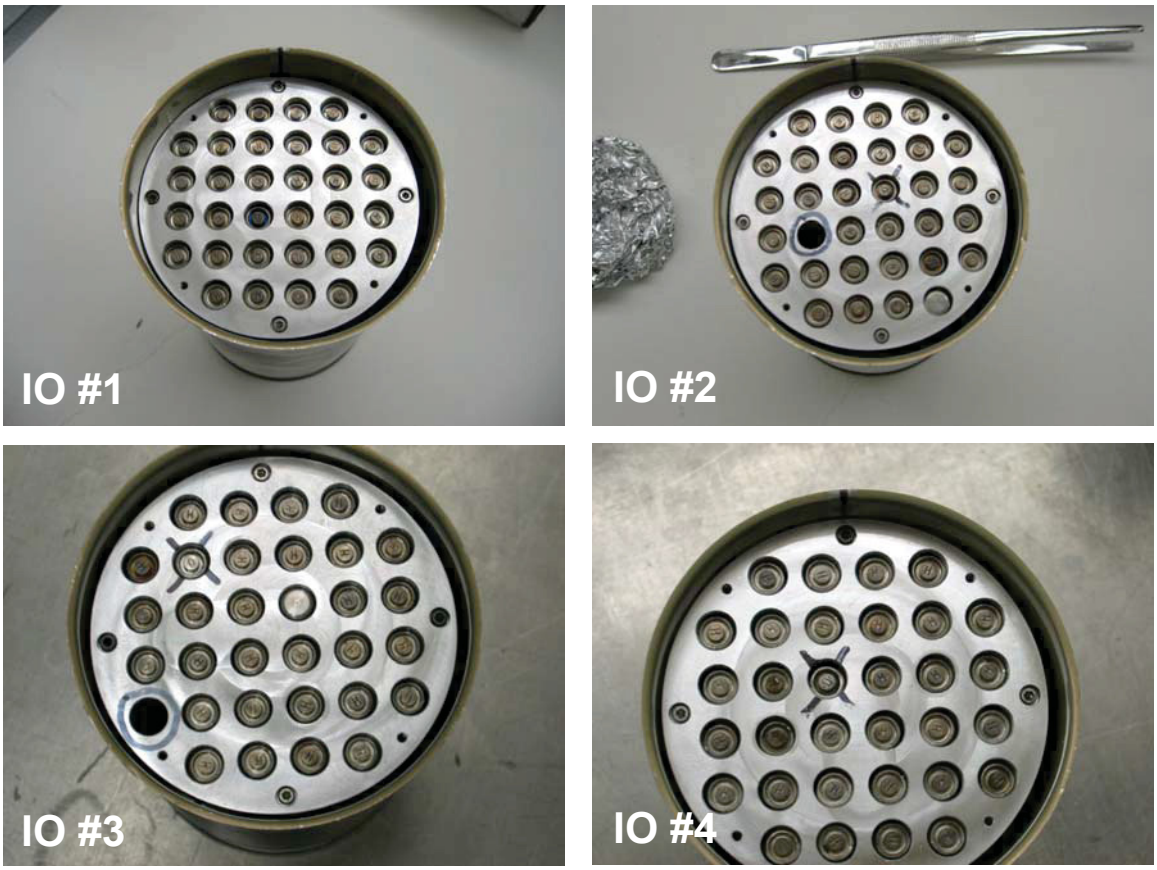


**Figure 35 The four inspection objects loaded with pins, prior to final assembly and sealing.**


**Figure 36 IO#1 before and after the crumpled aluminum has been put in place.**

## 5.3 ORNL Experiment Campaign

INL hosted researchers from ORNL in the final week of August, 2011 to perform these tests. Cost sharing was achieved by performing multiple experiments funded by different programs during the same week. Activities, in addition to the experiments, included arranging receipt and inspection of the ORNL shipping crates, unpacking the crates, assembling the equipment, testing the equipment, performing a radiological generating device inspection for the electronic neutron generator (ENG), disassembling the equipment, repackaging and re-crating the equipment, and arranging for shipment of the equipment out of INL at the end of the experiments. Some photographs from the experimental campaign are provided below.

- A photograph of some of the equipment staged on the floor of the ZPPR workroom, prior to assembly, is shown in Figure 37.
- A photograph of INL and ORNL staff assembling and testing the detector array for the experiment is shown in Figure 38.
- A photograph of the set-up used for initial neutron transmission scanning tests with the ENG, with the mock-up can, is shown in Figure 39.
- Photographs of IO#1 in the inspection zone of the radial collimator are shown in Figure 40 through Figure 43.


**Figure 37 ORNL equipment awaiting assembly in the ZPPR workroom.**


**Figure 38 Assembling the radial collimator detector array.**

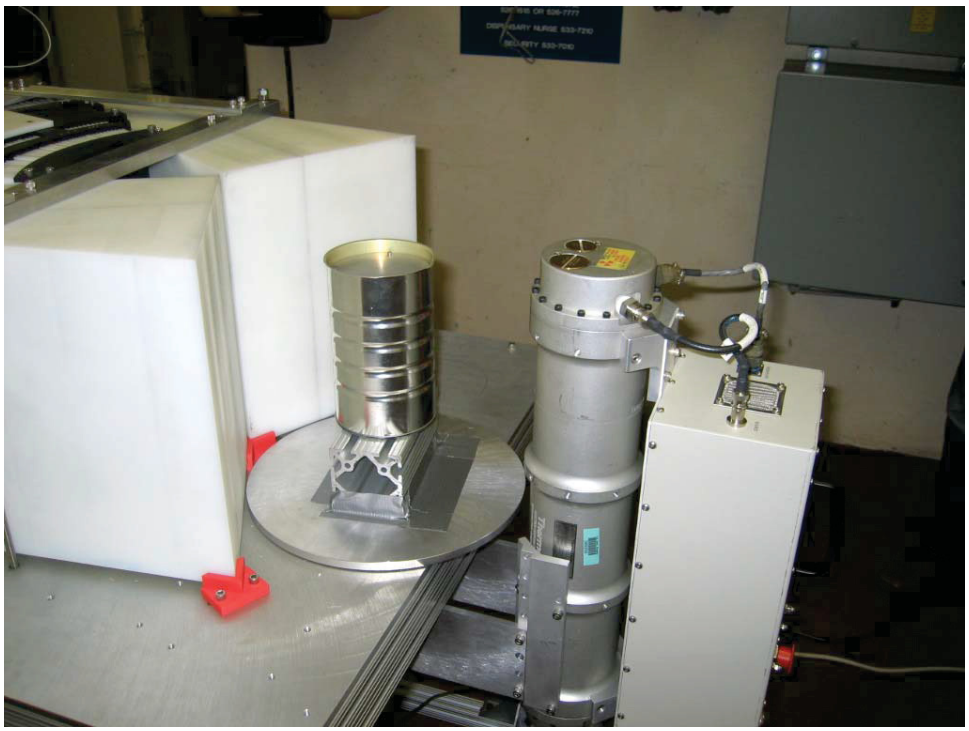

**Figure 39 Initial test configuration for neutron radiography using the ENG (right) and the mock-up can loaded with steel rods (middle).**


**Figure 40 Photograph of an inspection object in front of the radial collimator – end view.**

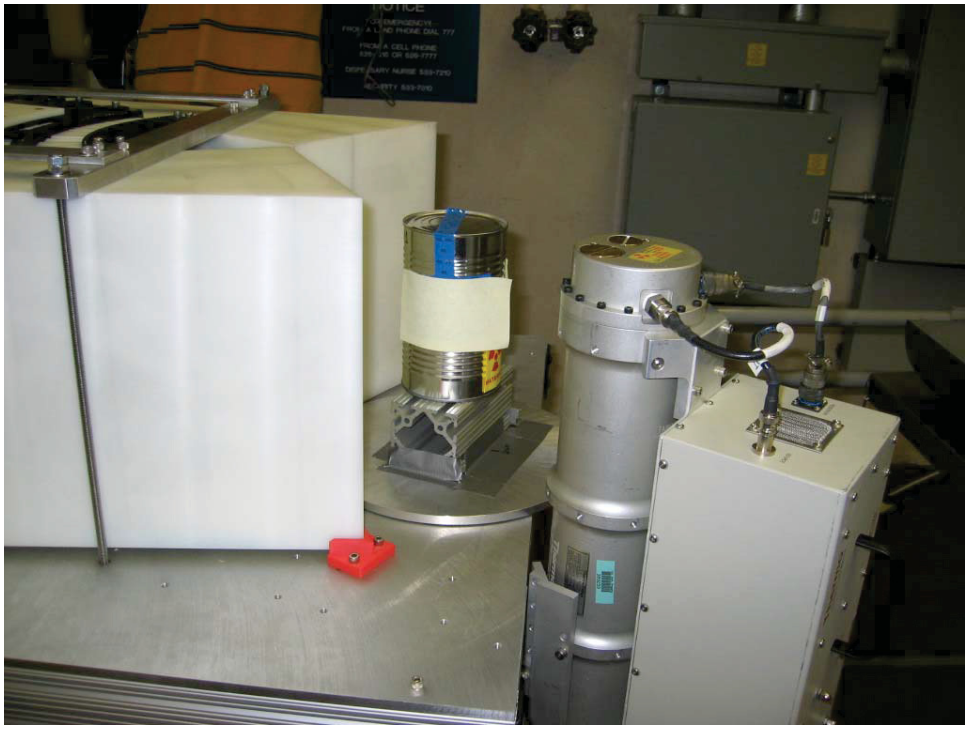

**Figure 41 Photograph of an inspection object in front of the radial collimator – side view.**

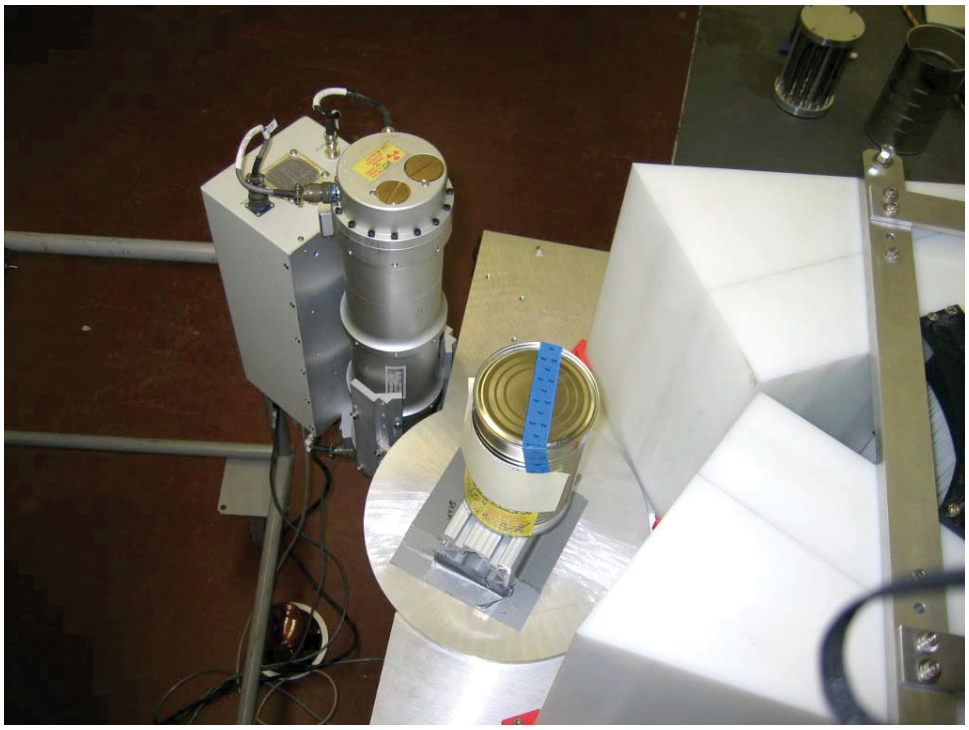

**Figure 42 Photograph of an inspection object in front of the radial collimator – top view.**

**Figure 43 Photograph of an inspection object in front of the radial collimator – top/side view.**

# 6 SUMMARY

The use of an AP-ENG, an AmLi neutron source, and LS detectors to perform TOF measurements as described in this report is the first time these different techniques have been brought together for nuclear material safeguards research and development. At this point only preliminary analyses have been performed for the large data set from the FY2011 experimental campaign at JRC-Ispra. Considering the interesting test materials used at JRC-Ispra, and the innovative combinations of passive and active neutron interrogation measurements that were performed there, many new safeguards-relevant measurement techniques may be examined using this data together with simulation and modeling. In FY2012, the INL-University of Michigan research collaboration will continue to refine the model fidelity representing the JRC-Ispra experiments and continue examining simulations with these models to interpret the data that was measured.

In response to new direction and needs of the MPACT program, in FY2012 the INL-University of Michigan MPACT collaboration will also begin focusing efforts towards the development, in FY2014, of a prototype fast-neutron time-correlation system for characterizing special nuclear materials and advanced fuel cycle materials relevant for the FCR&D program. For FY2012 this focused activity will consist primarily of a new science-based, engineering driven simulation and modeling effort to examine design features and trade offs for a LS-based neutron analysis system capable of operating in both passive and active neutron interrogation modes of operation. This work will involve the use of existing modeling software available at INL and the University of Michigan, including the advanced MCNP-PoliMi computer code supported by Prof. Pozzi and her team at the University of Michigan and the Polytechnico di Milano, and the development of software data-analysis tools to facility new numerical analyses as needed.

INL will also continue to work in collaboration with the ORNL team to develop new inspection objects for MPACT fast-neutron stand-off imaging applications, and work with the ORNL team to host future experimental activities using the ORNL instrumentation.

# 7 REFERENCES


1 Chichester, D. L., et al., "FY09 Advanced Instrumentation and Active Interrogation Research for Safeguards," Report INL/EXT-09-16611, Idaho National Laboratory, Idaho Falls, Id. (2009).

2 Looman, M., et al., "The Effect of Gadolinium Poison Rods on the Active Neutron Measurement of LEU Fuel Assemblies," Proc. 23rd ESARDA Annual Meeting, Bruges, Belgium, May 8-10 (2001) 568-573.

3 Chichester, D. L., Lemchak, M. and Simpson, J. D., "The API 120: A Portable Neutron Generator for the Associated Particle Technique," Nucl. Inst. Meth. Phys. Res. B 241 (753-758).

4 Tagziria, H., et al., "Measurement and Monte Carlo Modeling of the JRC $^{241}$Am-Li(a,n) Source Spectrum," Rad. Prot. Dos. 110 (2004) 129-134.

5 Padovani, E., et al., "Simulation of Correlated Counts from an Am-Li Source," Nucl. Inst. Meth. Phys. Res. A 557 (2006) 599-606.

6 Pozzi, S. A., et al., "Pulse-height Distributions of Neutron and Gamma Rays from Plutonium-Oxide Samples," Nucl. Inst. Meth. Phys. Res. A 608 (2009) 310-315.

7 Dolan, J. L., et al., "Nuclear Nonproliferation Measurements Performed on Mixed-Oxide Fuel Pins at the Idaho National Laboratory," Conf. Rec. IEEE Nucl. Sci. Symp., October 25-31 (2009).

8 Holewa, L. and Charlton, W., “Angular Anisotropy of Correlated Neutrons in Lab Frame of Reference and Application to Detection and Verification,” Inst. Nucl. Mat. Manag. 52nd Annual Meeting, Palm Desert, Calif., July 15-19 (2011).

9 Miller, E. C., et al., “Experiments and Simulation of Cross-Correlations on MOX Fuel,” Inst. Nucl. Mat. Manag. 52nd Annual Meeting, Palm Desert, Calif., July 15-19 (2011).

10 Chichester, D. L., et al., "Neutron Emission Characteristics of Two Mixed-Oxide Fuels: Simulations and Initial Experiments," Report INL/EXT-09-16566, Idaho National Laboratory, Idaho Falls, Id. (2009).

11 Chichester, D. L., Seabury, E. H., Turnage, J. A., Brush, B. A., and Perry, E. F., "Capabilities of the INL ZPPR to Support Active Interrogation Research with SNM," AIP Conf. Proc. 1099 (2009) 647-651.

12 Klann, R. T. Austin, B. D., Aumeier, S. E., and Olsen, D. N., "Inventory of Special Nuclear Materials from the Zero Power Physics Reactor," Report ANL-NT-176, Argonne National Laboratory-West, Idaho Falls, Idaho (2001).

# APPENDIX

This appendix contains the slides presented at the MPACT end-of-year meeting in Gaithersburg, Md., on September 14, 2011 (INL/MIS-11-2322).

INL/MIS-11-23222
*Approved for public release; distribution is unlimited.*

# Active Neutron Interrogation Fast Multiplicity Analysis

**David Chichester and Scott Watson (INL)**

**Sara Pozzi, Marek Flaska, and Jennifer Dolan (U. Michigan)**

**Paul Hausladen, Jason Newby, and Matthew Blackston (ORNL)**

Idaho National Laboratory

Detection for Nuclear Nonproliferation Group

Oak Ridge National Laboratory
MANAGED BY UT-BATTELLE FOR THE DEPARTMENT OF ENERGY

Idaho National Laboratory is a multiprogram laboratory operated by Battelle Energy Alliance for the United States Department of Energy under contract DE-AC07-05ID14517.

## Outline

- Project Background and Motivation
- Active Neutron Interrogation: Time of Flight (TOF) with a Time-Tagged ENG
- Active Neutron Interrogation: Low-energy Interrogation with AmLi
- Discussion
- Support for ORNL Imaging Activities
- Future Work
- Quad Chart

## Background

- In FY2011 this project was focused to:
  - Explore techniques for fast-neutron and photon correlation measurements, both passive and active.
  - Evaluate the use of a time-tagged DT neutron source, in conjunction with liquid scintillators, for characterizing special nuclear material.
- An extension of an FY2009 one-year collaboration (University of Michigan) to study advanced passive assaying methods.
- Our collaboration has been on small-scale studies, coupling simulation development and validation experiments, exploring fast-neutron measurement approaches with applicability for safeguards.

*Sara Pozzi, Jennifer Dolan, and Marek Flaska at INL in 2009 for the passive MOX fuel measurements.*

- FC R&D Objective:
  - Enhance overall nuclear fuel cycle proliferation resistance via improved technologies for used fuel management.
- MPACT Objective:
  - Improve the fundamental understanding of nuclear materials and the physics of detection methods through coupled theory, simulation, and experiment, as necessary to develop next-generation materials management and MPACT technology.

Chichester 3

## Motivation for MPACT

- **Looking forward, the project will now focused towards a more tangible, nearer-term outcome:**
  - Develop technique (measurement concept, instrumentation, and simulation) for using fast neutron multiplicity analysis with liquid scintillators-based multiplicity analysis as an approach for replacing helium-3 based instruments.
  - Develop and demonstrate a liquid-scintillator-based detection system for material accountancy measurements.
- Supporting and advancing the US DOE Domestic Nuclear Energy Program.

**US DOE "Nuclear Energy Research and Development Roadmap"**

**R&D Objective 4: Understand and Minimize the Risks of Nuclear Proliferation and Terrorism**

**Safeguards and Physical Security Technologies and Systems**

**Advanced Instrumentation**

- Development of advanced safeguards instrumentation such as active interrogation methods.
- Development of advanced passive detectors such as neutron multiplicity counting.

**Importance**

Material accountancy is a key part of domestic nuclear safeguards. Improved methods (faster, non-use of $^{3}$He, more versatile) are needed to support future domestic fuel-cycles.

**Results**

This project will demonstrate the use of fast-neutron multiplicity analysis with liquid scintillators and active interrogation for assaying fuel cycle materials.

**Innovation**

Current technology relies on $^{3}$He-based neutron detectors. This approach represents a new tool for MPACT measurements.

Chichester 4

## Prior Work from 2009 – INL & University of Michigan

- Simulation and modeling using MCNP-PoliMi.
- Passive measurements of INL MOX fuel.
  - Neutron and gamma-ray pulse shape discrimination.
  - Pulse-height distributions.
  - Time-correlated detections.
  - Multiplicity analysis.

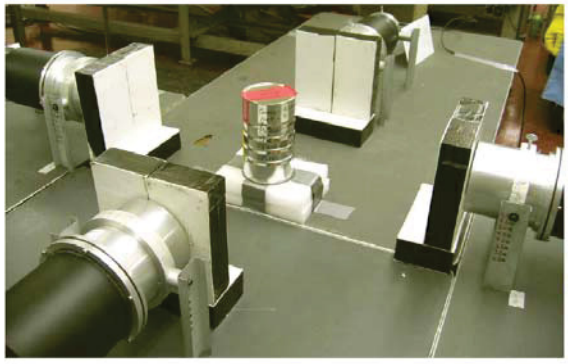



## 2011 – INL, University of Michigan, ORNL

- In 2011 our objective was to explore how active neutron interrogation may be coupled with liquid-scintillator based detectors for characterizing fissionable material for MPA&C measurements.
- Funding for this year did not support laboratory tests for this work at INL.
  - Prior INL-Michigan research (2009) has been of interest to colleagues at the European Commission's Joint Research Center (JRC) in Ispra, Italy (Paolo Peerani, PI).
  - For 2011 JRC-Ispra offered to host our research team and use their facilities.
  - We also accepted an offer from colleagues at the University of Padova (Giancarlo Nebia and Giuseppe Viesti) to borrow a time-tagged electronic neutron generator for this work
- In the winter and early spring of 2011 work focused on conceptual modeling to develop an experimental plan for our work at JRC-Ispra.
- Experiments took place at JRC-Ispra in May.
  - Detectors and data-acquisitions equipment were shipped to JRC-Ispra from the USA.
  - Tests focused primarily on uranium-bearing fuels (to emphasize using active interrogation).
    - Uranium-oxide powder: 1.5 kg (1% enrich.), 2.5 kg (3% enrich.), 2.5 kg (5% enrich.).
    - 17 x 17 PWR fresh-fuel assembly (3% enrich.).
- A second objective of INL work this year has been to support an ORNL-led experimental campaign to investigate advanced neutron imaging methods for analyzing MOX fuel assemblies.

## Our Test Campaign for FY2011

- In FY2011 we are extending the previous work using passive analysis and MOX fuel to the analysis of uranium with active neutron interrogation.
  - Active interrogation using a time-tagging, associated-particle neutron generator.
  - Benchmarking triple-level coincidences.
  - Equipment evaluation – digitizer performance.
  - $UO_2$ powder.
    - 1.5 kg; 1% enrichment
    - 2.5 kg; 3% & 5% enrichment
  - $UO_2$ full-scale, fresh-fuel assembly.
- Experiments using enriched $UO_2$ standards at JRC – Ispra.
  - Leveraging prior collaborative work between JRC-Ispra (PI: Paolo Peerani) and the University of Michigan.
  - Unique reference materials not available at INL.
  - Access to a prototype associated-particle (AP) electronic neutron generator (EADS SODERN) (PI: Giancarlo Nebbia, National Institute of Nuclear Physics (INFN), Italy).
  - Cost savings versus INL-sponsored experiments.

*European Joint Research Center (JRC) – Ispra, Italy*



## DT Active Interrogation: TOF Simulations

- Detectors
  - Five, 5"x5" liquid detectors
  - ~40 cm detector to source distance
- ENG neutron source
  - ~100 cm ENG-to-uranium distance
- Three $UO_2$ material samples
  - 1.5 kg, 1% enrichment
  - 2.5 kg, 3% enrichment
  - 2.5 kg, 5% enrichment
- MCNP-PoliMi tracks each particle and coincident particles based on origin as well as originating reaction.
- Prior benchmark/validation work has demonstrated the accuracy of the MCNP-PoliMi code for fission coincidence-type experiments.

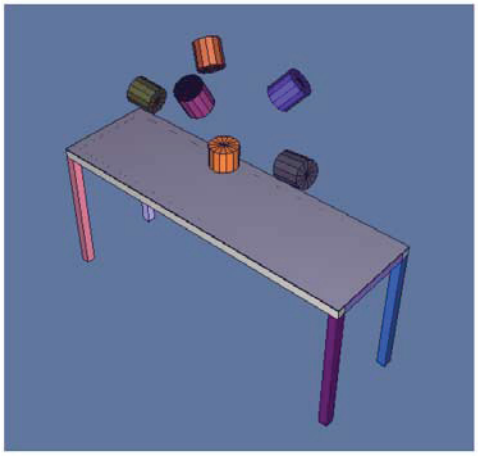

## DT Active Interrogation: Profiling the Beam



## DT Active Interrogation: Detector Set-up

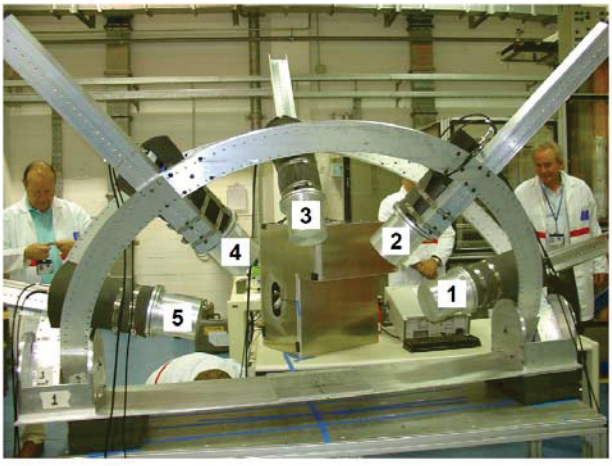

## DT Active Interrogation: Material Containers

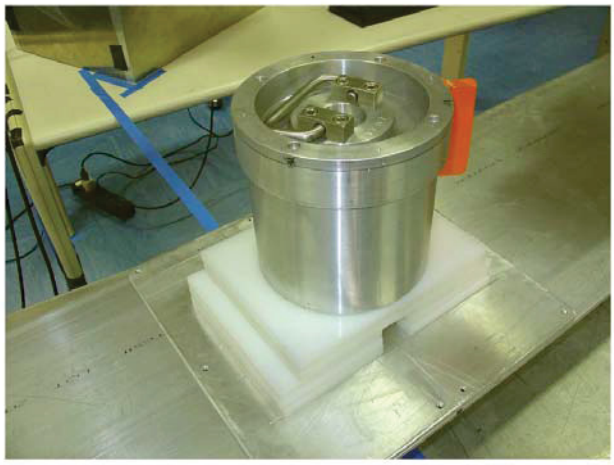



## DT Active Interrogation: Prelim. Sim. Tally Results

- Neutron current tally (F1) binned by neutron energy (10 keV bins), on each detector face.
  - Watt-like fission spectrum evident from 0 – 5 MeV.
  - Additional feature at 6 MeV and 11 MeV.
  - Scattered DT-source neutrons from 12-14 MeV.
- Liquids 1, 3, and 5 have scattered 14-MeV neutrons of lower energy entering the detector.
  - These three detectors are at greater scattering angles for 14-MeV neutrons incident on the sample.

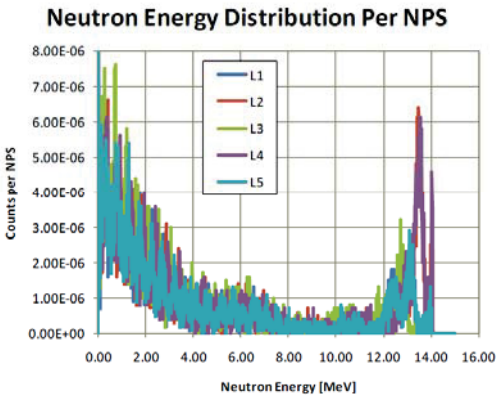

## DT Active Interrogation: Prelim. Sim. TOF Results

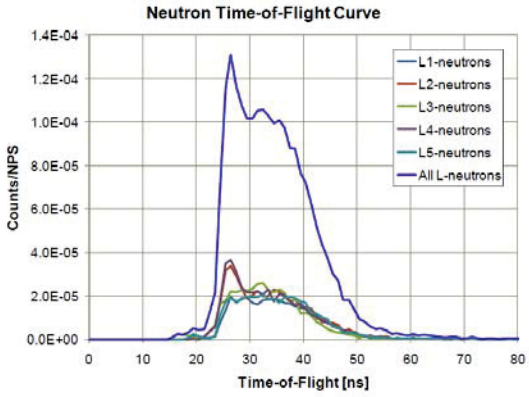


- LU44:2.5 kg, 5% enrichment.
- Individual detectors, simulated TOF curves with tagged-neutron source.
- Liquids 1, 3, and 5 have less obvious TOF contributions from the scattered 14-MeV neutron peaks: these three detectors require a greater scatter angle and therefore more neutron energy loss and a more distributed neutron energy distribution before detection
- Liquids 2 and 4 have a more significant 14-MeV scatter peak later in time



## DT Active Interrogation: Prelim. Sim. TOF Results

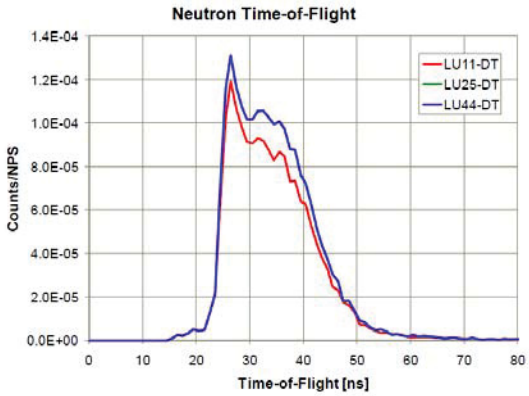


- Comparison of three LEU samples, simulated TOF curves with tagged-neutron source.
- LU11: 1.5 kg, 1% enrich.
- LU25: 2.5 kg, 3% enrich.
- LU44: 2.5 kg, 5% enrich.
- Only difference in mass is seen in the simulated TOF curve comparison.
- Difference is related to total U mass.

## DT Active Interrogation: Prelim. Exp. TOF Results

- Measurement Results
  - LU11: 1.5 kg, 1% enrich.
  - LU25: 2.5 kg, 3% enrich.
  - LU44: 2.5 kg, 5% enrich.
- The amount of scattered 14 MeV neutrons is similar for all three samples while the amount of neutron induced reactions differs significantly.
- As is seen in the simulations, the LEU samples with the same mass show the same TOF results with DT-interrogation. The lesser mass LEU sample shows fewer of its neutron detections in the induced fission region.
- DT ENG yield varied run-to-run and has yet be accounted for.

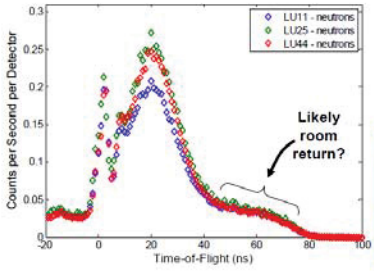


**Liq. Scint.**
$0.6<E_n<6$ MeV

∴ Timing is indicative of energy *but* pulse heights are not.

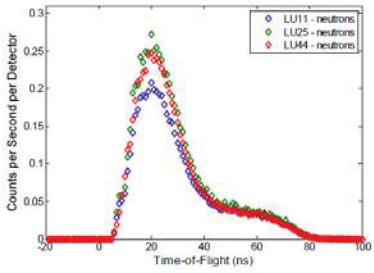




## DT Active Interrogation: Prelim. Sim. & Exp. TOF Results

**Simulation**

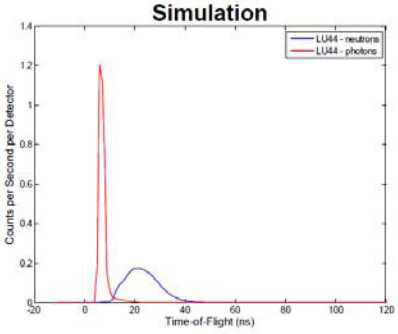


**Measurement**

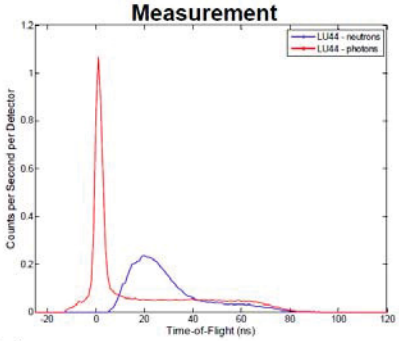


- Simulation validation: LU44: 2.5 kg, 5% enrich.
- Have accounted for the distance to the target and understand relative PMT timing capabilities.
- Need to account for YAP detector efficiency and threshold, for absolute comparison.

## AmLi Active Interrogation: Source and Moderation



## AmLi Active Interrogation: $UO_2$ Measurement

## MCNPX-PoliMi Event Results
### *Active Interrogation: Prelim. Event History*

- Many interesting trends
- Induced $^{238}U$ Fission
  - with DT, decreases with increased enrichment
  - with AmLi, increases with increased enrichment
- Induced $^{235}U$ Fission
  - always increases with enrichment
- (n,2n) and (n,3n) only significant with DT interrogation
- Inelastic scattering mostly prevalent with DT source neutrons

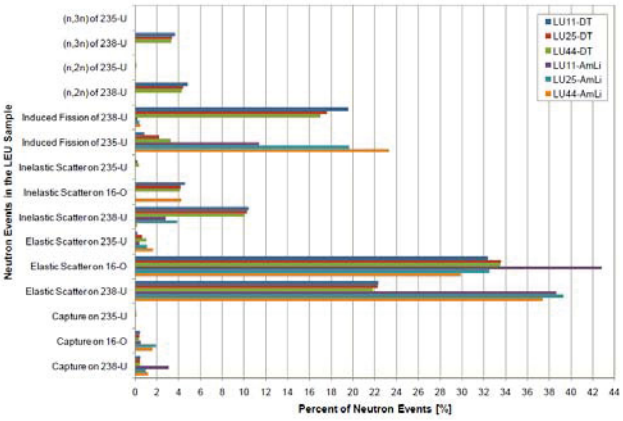




## Initial Observations

***Time-tagged DT active interrogation combined with AmLi interrogation.***

- Examining the fission-region of the DT TOF spectrum provides a measure of total uranium, while the AmLi measurement helps quantify the fissile fraction.
  - Similarities to active well counter, with added information about total uranium.
  - Suitable for unusual geometries, poorly defined/characterized geometry.
  - Potential for determining uranium enrichment as well as total mass.
  - Capable of penetrating through shields.
  - Potentially a low infrastructure measurement, could allow assay inside storage containers.
- TOF spectrum deconvolution holds promise for further data mining (isotopic differences for (n,n'), (n,2n), (n,3n), and fission-neutron energies).
- Time correlation with prompt gamma-ray neutron spectrometry may provide independent $^{16}O$ determination.
  - Differences in forward vs. backward elastic scattering.
  - Similar possibilities in fluorine may support extension to $UF_6$ enrichment assay.
- DT irradiation coupled with thermal neutron detection (vs. liquid scintillators) may eliminate need for AmLi, in die-away time region, with a pulsed ENG.
- The limited detector coverage of this experiment precluded adequate collection of neutron coincidence data adequate for determinations.

## AmLi Active Interrogation: Fuel Assembly Measurement



## Passive Measurements: Pu Metal Samples

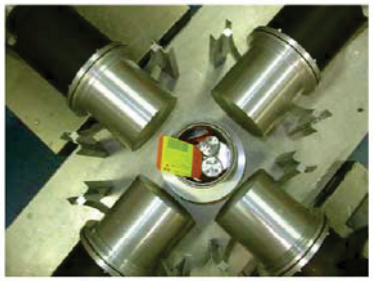

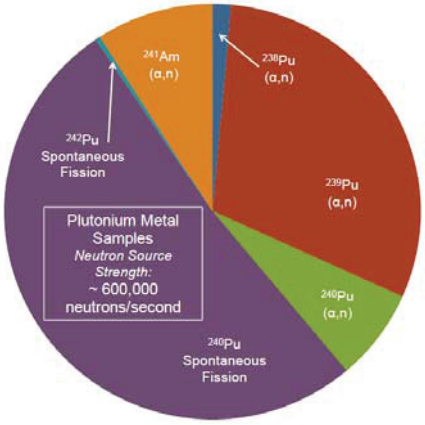

## Fission-Neutron Anisotropy

- At the most recent INMM meeting Laura Holewa (Texas A&M University) described using fission-neutron anisotropy as an additional constraining parameter in neutron coincidence analyses.
- Similar work was also presented by the University of Michigan, describing prior experiments at JRC-Ispra in this area.
- We have chosen to re-analyze data from our 2009 experiments at INL, as well as our recent JRC-Ispra experimental data, to explore this signature.

- Motivation
  - In neutron coincidence measurements it is important to be able to account for the fraction of uncorrelated neutrons ($\alpha$,n) versus correlated neutrons in the gross neutron count rate.
  - Scission of the fissioning nucleus leads to approximately 10% of prompt-fission neutrons, the remaining 90% are generated from the immediate decay of fission fragments.
  - Uncorrelated neutrons from ($\alpha$,n) reactions do not contribute to anisotropy measurements.
  - For well characterized measurement conditions, a measure of neutron-pair anisotropy using fast liquid scintillators may allow for differentiating the ($\alpha$,n) component.
  - Observed fission anisotropy may also provide insight related to material form, porosity, and density (fission-fragment range in mater).

Holewa, L. and Charlton, W., "Angular Anisotropy of Correlated Neutrons in Lab Frame of Reference and Application to Detection and Verification," Inst. Nucl. Mat. Manag. 52nd Annual Meeting, Palm Desert, Calif., July 15-19 (2011).
Miller, E. C., Dolan, J. L., Clarke, S. D., Flaska, M., Pozzi, S. A., Padovani, E., Peerani, P., and Schillebeeckx, "Experiments and Simulation of Cross-Correlations on MOX Fuel," Inst. Nucl. Mat. Manag. 52nd Annual Meeting, Palm Desert, Calif., July 15-19 (2011).



## Holewa's Equation

- Neutron Coincidence Counting
  - Contributions: spontaneous fission (SF), (α,n) (AN), induced fission (IF)
  - Singles Counts = Function of (SF rate, AN rate, IF rate)
  - Doubles Counts = Function of (SF rate, AN rate, IF rate)
  - Two equations, three unknowns

- Proposed new equation:

$$\frac{\text{Measured Frequency at } 180^{o}}{\text{Measured Frequency at } 90^{o}} = \frac{S_{180^{o}} \cdot (\text{SF rate} + \text{IF rate}) + X}{S_{90^{o}} \cdot (\text{SF rate} + \text{IF rate}) + X}$$

$S_{180^{o}}$ = Normalized simulated frequency at $180^{\circ}$

$S_{90^{o}}$ = Normalized simulated frequency at $90^{\circ}$

$X = \text{AN rate} \cdot \varepsilon^{2}$

$\varepsilon$ = Detector efficiency

Holewa, L. and Charlton, W., "Angular Anisotropy of Correlated Neutrons in Lab Frame of Reference and Application to Detection and Verification," Inst. Nucl. Mat. Manag. 52nd Annual Meeting, Palm Desert, Calif., July 15-19 (2011).

## Passive Measurements
### *2011 JRC Ispra Facility – Pu Metal Samples*

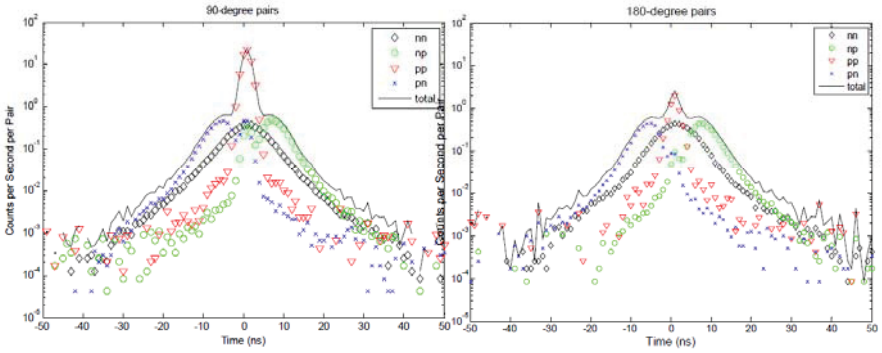




## Passive Measurements
### *2011 JRC Ispra Facility – Pu Metal Samples*

- Three small Pu Metal samples
  - Total Pu mass:
  - 1 cm of lead shielding
- Ratio of 180/90 degree correlated neutron detections = 1.14

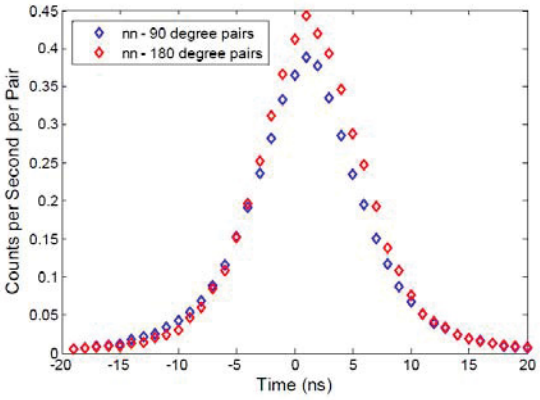

## Passive Measurements
### *2009 INL ZPPR Facility – MOX Fuel Pins*

- 90-pin can of MOX fuel
  - Type 127
  - Low Pu-240 content
  - 5 cm of lead shielding
- Ratio of 180/90 degree correlated neutron detections = ~1.25 ± ?
- Ratio of spontaneous fission neutrons to (α,n) neutrons = 1.27

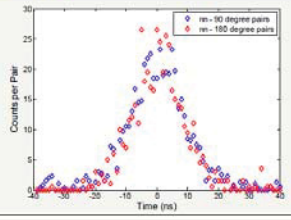


- 90-pin can of MOX fuel
  - Type 129
  - High Pu-240 content
  - 5 cm of lead shielding
- Ratio of 180/90 degree correlated neutron detections = ~1.31 ± ?
- Ratio of spontaneous fission neutrons to (α,n) neutrons = 1.59

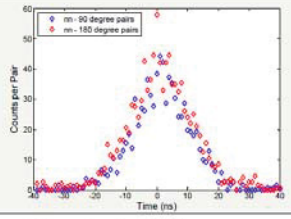


***Note: The SF neutron source has more neutrons below the LS cut-off than the (α,n); this energy-dependent efficiency degrades the observed SF: (α,n) anisotropy. Further work is need et to quantity this.***

Chichester 27

## Support to ORNL for Fast-Neutron Imaging R&D

- Within the Fuel Cycle R&D program ORNL (Paul Hausladen, PI) is working to develop advanced fast-neutron imaging methods applicable for material protection, accountancy, and control.
- INL has supported these efforts since 2009, hosting the team for performing measurements with uranium and plutonium.
  - First round testing focused on proof-of-concept imaging.
  - High gamma-ray emission rate of MOX fuel ($^{241}$Am) and facility background radiation fields have motivated research to develop liquid-scintillators-based detectors (vs. plastic scintillators).

***ORNL/INL experiments at INL's ZPPR facility in 2009.***

*Bundle of 9 fuel pins arranged in an "I" formation within a steel case.*

Chichester 28

## Nuclear Material at INL

***Access to products from all stages of the fuel cycle***


Also: Aqueous reprocessing wastes and process streams, actinide fuel fabrication products and wastes, ceramic waste forms, low-level waste drums, Idaho chemical plant wastes, TRU waste drums, commercial spent reactor fuel, commercial spent fuel in dry fuel storage casks, DOT approved spent fuel transportation casks, …




## Development of the MOX Fuel-Pin Inspection Objects

- In August of 2011 INL hosted Paul Hausladen from ORNL for an experiment campaign evaluating methods for performing fast-neutron tomography of mixed-oxide fuel for material accountancy.
- INL assembled four inspection objects (IOs) with square-array assemblies of MOX fuel pins.
  - 32 pin locations per IO.
  - High burn up Pu (26% $^{240}$Pu isotopic).
  - One IO with full MOX load.
  - Three cans with single-pin missing.
  - Complications due to void, stainless steel replacement, depleted-uranium replacement.
- IOs assembled in July, 2011.
- Testing took place at INL's ZPPR test facility.

*Rendering of the Fuel-Pin Inspection Objet Geometry.*

## IO Pin Loadings

Idaho National Laboratory

*Seam on each can is at top of each image.*

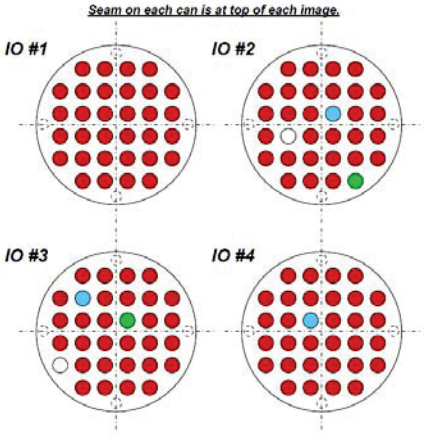


- PUOH, Vendor 80, ID No. 129 (~26% $^{240}$Pu)
- UODR, ID No. 130 (0.2% $^{235}$U)
- Stainless Steel, 304 (supplied with can inserts)
- Empty

UODR
ID No. 130
(0.2% $^{235}$U)

| ID Symbol | UODR |
|---|---|
| ID No. | 130 |
| Size | 3/8 in. d.* x 6 in. long |
| Average weight | 102.941 |
| Core weight | 89.787 |
| 88.106 wt% Fe | 79.107 |
| $^{235}$U | 0.159 |
| $^{238}$U | 78.948 |
| 11.852 wt% O | 10.642 |
| 0.042 wt% Other | 0.038 |
| Clad weight | 12.392 |
| 69.53 wt% Fe | 8.617 |
| 18.54 wt% Cr | 2.298 |
| 9.65 wt% Ni | 1.196 |
| 1.28 wt% Mn | 0.159 |
| 0.47 wt% Si | 0.058 |
| 0.09 wt% Co | 0.011 |
| 0.06 wt% Mo | 0.007 |
| 0.06 wt% Cu | 0.007 |
| 0.03 wt% Ti | 0.006 |

PUOH, Vendor 80,
ID No. 129
(~26% $^{240}$Pu)

| Description | Vendor 80 15% Pu High 240 |
|---|---|
| ID Symbol | PUOH |
| ID No. | 129 |
| Size | 3/8 in. d.* x 6 in. long |
| Average weight | 102.6926 |
| Core weight | 89.7368 |
| Pu weight | 14.0147 |
| $^{238}$Pu | 0.0096 |
| $^{239}$Pu | 9.8079 |
| $^{240}$Pu | 3.6603 |
| $^{241}$Pu | 0.3170 |
| $^{242}$Pu | 0.0200 |
| $^{241}$Am | 0.1473 |
| U weight | 64.5949 |
| $^{235}$U | 0.1391 |
| $^{238}$U | 64.4458 |
| O | 10.5916 |
| Clad weight | 12.39 |
| 69.53 wt% Fe | 8.615 |
| 18.54 wt% Cr | 2.297 |
| 9.65 wt% Ni | 1.196 |
| 1.28 wt% Mn | 0.159 |
| 0.47 wt% Si | 0.058 |
| 0.09 wt% Co | 0.011 |
| 0.06 wt% Mo | 0.007 |
| 0.06 wt% Cu | 0.007 |
| 0.03 wt% Ti | 0.006 |

***Materials needed:***
PUOH → 32 +29 + 29 +31 = 121 pins
UODR → 3 pins
Stainless steel → 2 pins



## IO Assembly

Idaho National Laboratory


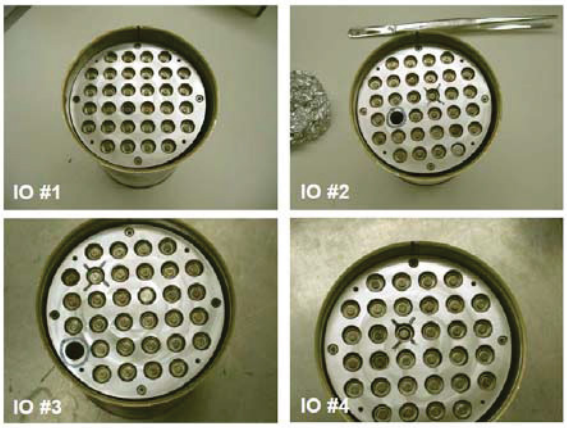

## Future Work

- Continue analysis of 2011 experimental data.
- Switch emphasis from exploration (methods development, simulation tools development, signature exploration and understanding) to an instrumentation design and development project.
- FY2012: Simulation and modeling to support development of a fast-neutron multiplicity analysis prototype.
  - Extensive prior benchmarking experiments with MCNP-PoliMi gives a high level of confidence in the simulation campaign.
  - Define instrument requirements.
  - Define parameter space for models.
  - Trade study vs. other technologies.
  - Simulate expected performance capabilities.
- Continue advanced studies, at reduced level of effort.
  - Combined neutron-photon correlation analysis.
  - Anisotropy analysis.
- Publish results.



## Publications and Presentations

Enqvist, A., Flaska, M., Dolan, J. L., Chichester, D. L., and Pozzi, S. A., "A Combined Neutron and Gamma-Ray Multiplicity Counter Based on Liquid Scintillation Detectors," Nucl. Inst. Meth. Phys. Res. A., In Press (2011).

Dolan, J. L., Flaska, M., Pozzi, S. A., and Chichester, D. L., "Comparison of Passive Measurements on Well-Described Mixed-Oxide Fuel Pins for Nuclear Safeguards Applications," Amer. Nucl. Soc. Trans. 103, Winter (2010).

Hausladen, P. A., Blackston, M. A., and Chichester, D. L., "Passive and Active Coded-Aperture Imaging of Fission-Spectrum Neutron Sources," IEEE Nuclear Science Symposium, Knoxville, Tenn., October 30 - November 5 (2010).

Chichester, D. L. and Watson, S. M., "Multispectral UV-Visual Imaging as a Tool for Locating and Assessing Ionizing Radiation in Air," IEEE Nuclear Science Symposium, Knoxville, Tenn., October 30 - November 5 (2010).

Chichester, D. L., Seabury, E. H., Wharton, J., and Watson, S. M., "INL Neutron Interrogation R&D: FY2010 MPACT End of Year Report," Report INL/EXT-10-19685, Idaho National Laboratory, Idaho Falls, Id. (2010).

Dolan, J. L., Flaska, M., Pozzi, S. A., and Chichester, D. L., "Measurement and Characterization of Advanced Nuclear Fuels at the Idaho National Laboratory Through Neutron Spectrum Unfolding," Inst. Nucl. Mat. Manag. 51st Annual Meeting, Baltimore, Md., July 11-15 (2010).

Dolan, J. L., Flaska, M., Pozzi, S. A., and Chichester, D. L., "Methods of Identification and Characterization of Mixed-Oxide Fuels Through Passive Measurement," 2010 ANS National Student Conference, Ann Arbor, Mich., April 8 – 11 (2010).

Dolan, J. L., Flaska, M., Pozzi, S. A., and Chichester, D. L., "Nuclear Nonproliferation Measurements Performed on Mixed-Oxide Fuel Pins at the Idaho National Laboratory," IEEE Nucl. Sci. Symp. Conf Rec., (2009) 925-930.

Chichester, D. L., Pozzi, S. A., Seabury, E. H., Dolan, J. L., Flaska, M., Johnson, J. T., Watson, S. M., and Wharton, J., "FY09 Advanced Instrumentation and Active Interrogation Research for Safeguards," Report INL/EXT-09-16611, Idaho National Laboratory, Idaho Falls, Id. (2009).

Chichester, D. L., Pozzi, S. A., Dolan, J. L., Flaska, M., Johnson, J. T., Seabury, E. H., and Gantz, E. M., "Neutron Emission Characteristics of Two Mixed-Oxide Fuels: Simulations and Initial Experiments," Report INL/EXT-09-16566, Idaho National Laboratory, Idaho Falls, Id. (2009).

Dolan, J. L., Flaska, M., Pozzi, S. A., and Chichester, D. L., "Passive Measurement and Characterization of Mixed-Oxide Fuel Pins at The Idaho National Laboratory," Inst. Nucl. Mat. Manag., Central Chapter 2009 Fall Meeting, Oak Ridge, Tenn., November 3 – 4 (2009).

Dolan, J. L., Flaska, M., Pozzi, S. A., and Chichester, D. L., "Comparison of Passive Measurements on Well-Described Mixed-Oxide Fuel Pins for Nuclear Safeguards Applications," Nuclear Science Symposium and Medical Imaging IEEE Conference, Orlando, Fla., October 25 – 31 (2009).

Hausladen, P. and Blackston, M., "Passive and Active Fast-Neutron Imaging in Support of AFCI Safeguards Campaign," Report ORNL/TM-2009/210, Oak Ridge National Laboratory, Oak Ridge, Tenn. (2009).

Dolan, J. L., Flaska, M., Pozzi, S. A., and Chichester, D. L., "Measurement and Characterization of Nuclear Material at Idaho National Laboratory," J. Nucl. Mat. Manag. 38 (2009) 40-47.

## Fast Neutron Multiplicity Analysis – *Quad Chart*

*Four large liquid scintillator detectors are shown here being used to analyze a storage can of MOX fuel pins.*

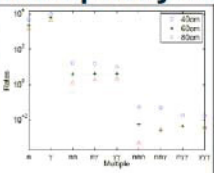

*Observed singles, doubles, and triples count rates from the MOX fuel shown to the left.*

***POCs: David Chichester (INL), Sara Pozzi (U. Michigan), Paul Hausladen (ORNL)***

***Statement of the MPACT Need:***
***Alternatives to existing helium-3 based neutron detection are needed. This project is examining the potential benefits of combining active neutron interrogation with liquid scintillator-based multiplicity analysis techniques.***
***Key Outcomes:***
***Develop and demonstrate the use of active neutron interrogation to improve multiplicity analysis measurements; also support ORNL testing of neutron imaging***

Technical Challenges

- Using digital pulse shape analysis with active interrogation for multiplicity analysis and the use of active multiplicity counting with liquid scintillators in this context.
- Developing a modeling framework with sufficient fidelity to accurately simulate higher-order interrogation coincidences.
- Satisfactorily dealing with and recovering from neutron generator bursts to collect data in-between neutron pulses.

FY2011 Planned Accomplishments

- Develop a comprehensive, time-dependent modeling & simulation framework to evaluate time-correlated liquid scintillator response measurements for active neutron interrogation multiplicity analysis.
- Carry out benchmark experimental measurements of active neutron interrogation multiplicity analysis using nuclear fuel.
- Evaluate the feasibility and benefits of using active neutron interrogation multiplicity analysis.
- Support ORNL fast neutron imaging experiments at INL.

*Five-Year Focus: Prototype demonstration for mixed transuranics (TRL-6) in 2014*



**INL/MIS-11-23222**
*Approved for public release, distribution is unlimited.*

# Active Neutron Interrogation Fast Multiplicity Analysis

**David Chichester and Scott Watson (INL)**

**Sara Pozzi, Marek Flaska, and Jennifer Dolan (U. Michigan)**

**Paul Hausladen, Jason Newby, and Matthew Blackston (ORNL)**

***For further information contact me at:***
Nuclear Nonproliferation Division
Idaho National Laboratory
2525 North Fremont Avenue
Idaho Falls, Idaho 83415
david.chichester@inl.gov
208-526-8920 & 208-526-9810

Idaho National Laboratory is a multiprogram laboratory operated by Battelle Energy Alliance for the United States Department of Energy under contract DE-AC07-05ID14517.